PERGAMON

Journal of Geodynamics 33 (2002) 281–314

JOURNAL OF GEODYNAMICS

www.elsevier.com/locate/jgeodyn

Numerical modelling of PT-paths related to rapid exhumation of high-pressure rocks from the crustal root in the Variscan Erzgebirge Dome (Saxony/Germany)

A.P. Willner[a,*], E. Sebazungu[b], T.V. Gerya[a,c], W.V. Maresch[a], A. Krohe[d]

[a]*Institut für Geologie, Mineralogie und Geophysik, Ruhr-Universität, D-44780 Bochum, Germany*
[b]*Institut für Geowissenschaften (Geophysik), Universität Mainz, D-55099 Mainz, Germany*
[c]*Institute of Experimental Mineralogy, Russian Academy of Sciences, Chernogolovka, Moscow district, 142432 Russia*
[d]*Institut für Mineralogie, Universität Münster, Corrensstr. 24, D-48149 Münster, Germany*

Received 10 September 2001; received in revised form 11 October 2001; accepted 11 October 2001

Abstract

The Bohemian Massif in the Central European Variscides contains many crustal slices with (ultra-)high-pressure rocks related to continent-continent collision. After closure of pre-existing oceans during the Devonian, excess crustal thickness was maintained for about 50 Ma until at around 340 Ma large volumes of high-pressure rocks from the crustal root were exhumed within a few million years. We relate this event to delamination and complete detachment of the lithospheric mantle, causing a crustal-scale isostatic instability. In the Erzgebirge dome, a model region in the northern part of the massif, an array of inter-related PTtd-paths with "decompression/cooling" and "decompression/heating" trajectories in juxtaposed tectonometamorphic units has been established. Numerical 2D-experiments using a rheologically, thermally and dynamically consistent convection technique show three stages of the crustal evolution related to delamination and detachment of mantle lithosphere under the crustal root: (1) During delamination a rapid overthickening of the crust can occur with the crust penetrating down to >160 km depth. (2) After detachment extensional crustal thinning controlling exhumation occurs with escape of rocks from the crustal root towards the margins of the orogen through tectonically weak zones. Horizontal displacement exceeds vertical by a factor of ~ 3. (3) Forced circulation in the weak zones follows and upward flow of lower crustal rocks is compensated by subduction of upper crustal rocks in the footwall of these zones. One-dimensional modelling was used in order to further understand basic processes and to simulate the rock record in detail. According to 2D and 1D modelling, strongly decelerating exhumation rates with decreasing overburden and a late increase in the geothermal gradient due to upward heat transfer are necessary corollaries of this scenario, in keeping with observations from the Erzgebirge dome. Exhumation

* Corresponding author. Fax: +49-234-321-4433.
E-mail address: arne.willner@rz.ruhr-uni-bochum.de (A.P. Willner).

PII: S0264-3707(01)00071-0

PT-paths do not conform to one single uniform exhumation trajectory; rather, assemblages of interrelated PTtd-paths are characteristic.

1. Introduction

In the past decade there has been a growing interest in the role of tectonic processes leading to the exhumation of high- and ultra-high-pressure crustal rocks during and following continent-continent collision. New models explaining exhumation have been derived from the pressure-temperature-time-deformation-paths of small crustal units by integrating structural, metamorphic and geochronological data. Various forward-modelling techniques have been developed to further constrain and understand established crustal dynamic models in specific well-studied model regions. The importance of continental convergence on the one hand and related delamination and detachment of lithospheric roots beneath collisional orogens on the other hand has been widely recognized in numerous studies and extensively studied theoretically, including 2D numerical geodynamic modeling (e.g. Bird, 1978; Houseman et al., 1981; Houseman and England, 1986; Sandiford and Powell, 1990; Zhou and Sandiford, 1992; Platt and England, 1993; Stüwe and Sandiford, 1995; Batt and Brown, 1997; Stüwe and Barr, 1998; Schott and Schmeling, 1998; Koyi et al., 1999; Schott et al., 2000; Arnold et al., 2001). Such studies have established the major features of the dynamics and the thermal regime of converging continental crust and lithospheric mantle and have delineated the physical characteristics and the timing of detachment of the lithospheric roots. However, with a few exceptions (e.g. Stüwe and Sandiford, 1995; Stüwe and Barr, 1998) the dynamics of exhumation and the corresponding PTt-paths of the crustal rocks involved in the crustal thinning (e.g. Schott and Schmeling, 1998) postdating detachment of the lithospheric roots have not been addressed in great detail.

A P–T-time path is a direct record of the movement of a rock within the Earth's crust during the process of metamorphism and thus represents a powerful tool for understanding the geodynamics of metamorphic terrains (e.g. England and Thompson, 1984; Perchuk, 1989; Spear, 1993; Perchuk et al., 1999; Willner et al., 2000). Hence, further efforts are needed to link the results from theoretical studies of delamination and detachment of lithospheric roots to the natural record on the P–T-time-deformation histories of metamorphic rocks in collisional orogens. This is especially important for correctly deciphering the tectonic development of those metamorphic terrains for which delamination and detachment are recognized as major geodynamic processes (e.g. Bird, 1978; Stüwe and Sandiford, 1995; Zulauf, 1997; Schott and Schmeling, 1998; Willner et al., 2000). One of the most interesting natural example of such terrains is found in the Bohemian Massif of the Mid-European Variscides belt.

The Mid-European Variscides belt is a well-documented collisional orogen assembled between about 420 and 300 Ma. Its southeastern part, the Bohemian Massif, represents a collage of crustal slices from very different crustal depths, including abundant high- and ultra-high-pressure rocks (various gneisses, high-pressure granulites, eclogites, garnet peridotites, Fig. 1) which suggest subduction of crustal material to mantle depths of 100–160 km and emplacement of mantle material. This part of the orogen, however, is presently characterized by a very thin overall lithospheric thickness of only 50–60 km (Mengel, 1992), and several authors explain this as a result of a detachment of the lithospheric root (Zulauf, 1997; Schott and Schmeling, 1998; Willner et al., 2000).

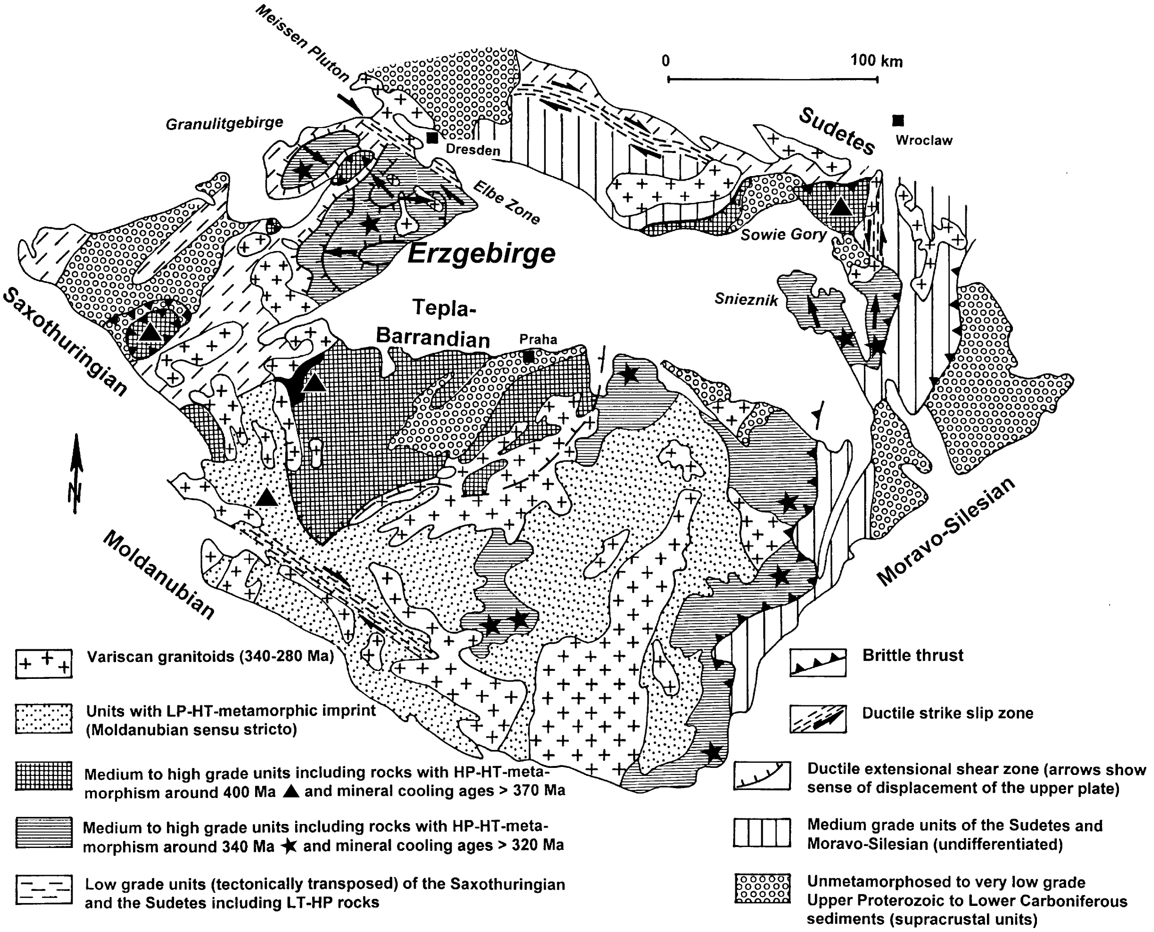

Fig. 1. Major geological features of the Bohemian Massif. The Erzgebirge dome is located in the NW. For a compilation of age data see Kröner and Willner (1998).

Schott and Schmeling (1998) extensively studied such a scenario with 2D numerical experiments and established the major physical controls of delamination/ detachment regimes describing the general sequence of tectonic events involved. They showed that the negative buoyancy forces of a lithospheric root may cause lateral shortening, whereby the lithospheric root then delaminates from the crust, detaches, and is replaced by hot upwelling asthenosphere. This provides a large input of heat into the crust. The late orogenic phase may therefore be characterized by extension, high heat flow, high temperature- low pressure metamorphism and a rapid (within a few million years) increase of the topography. However, the numerical experiments of Schott and Schmeling (1998) were not aimed at addressing in great detail the dynamics of the crustal rocks themselves. Comprehensive databases on the tectonic and P–T-deformation histories of metamorphic complexes within the Bohemian Massif are available (e.g. O'Brien and Carswell, 1993; Krohe, 1998; Willner et al., 2000). Comparison with numerical modelling should lead to a better understanding of the details of the delamination process. Another important problem that should also be addressed using the numerical modelling approach is related to the recent discovery of diamond-bearing quartzo-feldspathic rocks (Massonne, 1999; Stöckhert et al., 2001) exposed in the Erzgebirge of the northern Bohemian Massif (Fig. 2). The formation and exhumation of these rocks from ~160 km depth requires an adequate tectonic explanation and a link to the major geodynamic processes operating during delamination of the lithospheric root.

Therefore, the principal goal of the present paper is to address the relationship between delamination and detachment of the mantle lithosphere and the dynamics of the high- to ultrahigh-pressure metamorphic rocks from the crustal root with numerical modelling. Our study intends to extract relevant detailed information from numerical experiments such as characteristic P–T paths, variation of exhumation velocities and the amount of horizontal and vertical movements, in order to compare these with the petrological and geological information from the Bohemian Massif, in particular from the Erzgebirge dome (Fig. 2), which may be regarded as an excellent model region for studying the formation and exhumation of high- to ultra-high-pressure metamorphic rocks.

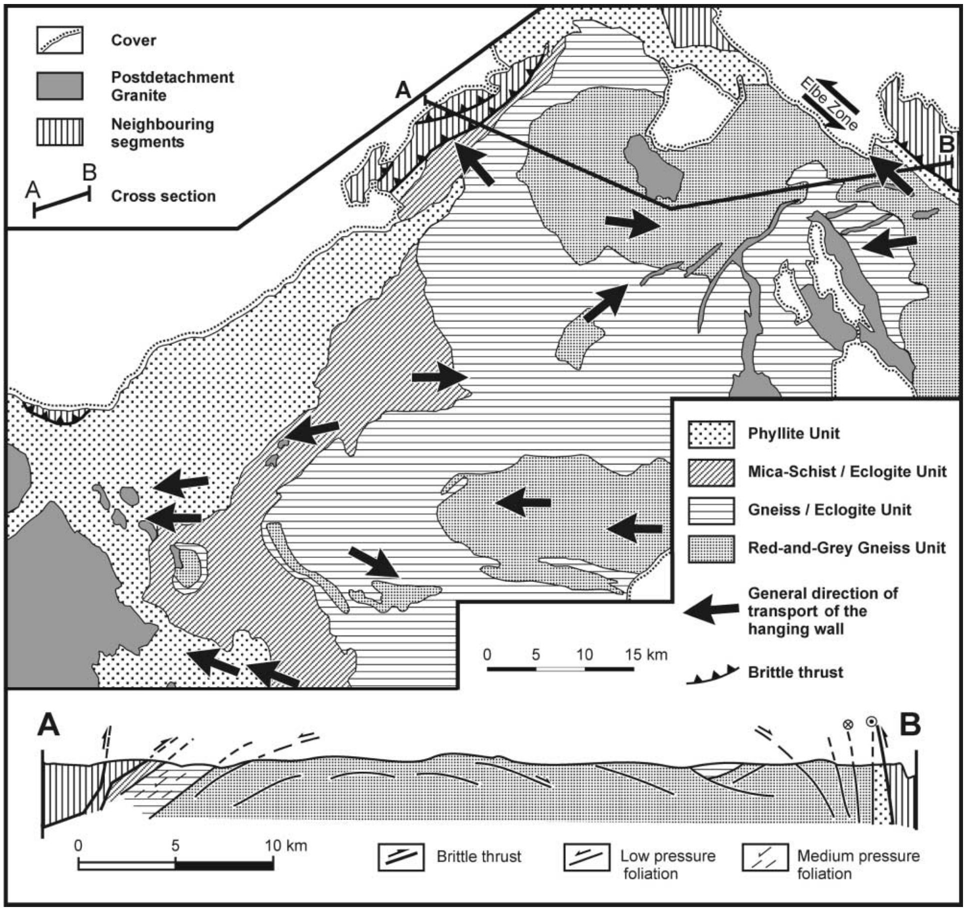

Fig. 2. Generalized geological map of the Erzgebirge dome with a cross section. For more details see Willner et al. (2000). Vertical exaggeration in the section is four times.

2. Regional geological framework and the delamination model

Tectonic slices of high- and ultra-high-pressure rocks occur scattered throughout the entire Bohemian Massif (Fig. 1, for a review see O'Brien and Carswell, 1993). Within this central zone of the Mid-European Variscides (part of the so-called "Moldanubian zone"), most of the crustal thickening occurred during Early Devonian collision between the Gondwana-derived "Armorica" and "Avalonia" plates. The age of high-pressure metamorphism ranges from 420 Ma to a predominant 340 Ma (cf. Kröner and Willner, 1998; Kröner et al., 2000a,b for summary). It is commonly accepted that closure of the oceans in the central part of the Variscides occurred in the Devonian (see Zulauf, 1997; Krohe, 1998), as indicated for example by the 400 Ma age for high-pressure metamorphism and coeval deposition of synorogenic greywackes into the adjacent part of the marine Saxothuringian basin in the north. However, orogenic activity continued for more than 100 Ma as an intraplate process, and no well-defined suture zone can be detected. In fact, the centre of the Mid-European Variscides is characterised by a destroyed orogenic wedge, i.e. a collage of crustal slices of very different geodynamic evolution exhumed from different depths (Fig. 1). An additional important feature is an extensive, late, regional high-temperature/low-pressure metamorphic overprint in the exposed lower tectonic levels, and S-type granitic magmatism between about 330 and 320 Ma that is generally regarded as characteristic of the "Moldanubian zone" (see Fig. 1).

Delamination of the lithospheric root after 340 Ma has been proposed to explain these features (e.g. Zulauf, 1997), as well as the preservation of the Tepla-Barrandian block (Fig. 1) in the centre of the Bohemian Massif. This is a large upper-crustal block which overlies the Moldanubian and still contains structures mainly related to Mid-Devonian crustal stacking as well as metamorphic rocks exhumed before 370 Ma. The Bohemian Massif represents the area with the maximum initial crustal thickness after the Variscan orogeny. At present it is still characterized by the greatest present crustal thickness of about 36 km, but also by the lowest overall lithospheric thickness of about 50–60 km (Mengel, 1992). The age of the metamorphic peak of most high-pressure rocks in the northern and southern part of the Bohemian Massif is around 340 Ma (see summary of data in Kröner and Willner, 1998; Kröner et al., 2000a,b). Mineral cooling ages are only slightly younger. On the basis of these data, Willner et al. (2000) proposed a conceptual model in which a thickened crustal bulge existed in the Mid-European Variscides for about 50–60 Ma after closure of the oceans and continent-continent collision, followed by its sudden destruction with concomitant crustal stretching and exhumation of slices from the crustal root at 340 Ma within a few million years (Fig. 3). A substantial buoyancy instability due to the detachment of the lithospheric root is believed to have triggered exhumation (extrusion) of rocks from the crustal root within a broad "channel-like" zone between the subsiding marine Saxothuringian basin and the heterogeneous upper-crustal Tepla-Barrandian block (Fig. 3), causing forced internal convection within the crust. This conceptual model suggests (i) a penetrative compressional deformation during subduction and stacking in the lower part of the convection zone at the prograde metamorphic stage and (ii) penetrative extensional deformation in the upper part during exhumation and unroofing at the retrograde metamorphic stage. The latter imprint dominates most rocks of the Erzgebirge dome. Although this basic principle is also proposed in many other accepted current models, such as those of Ernst and Peacock (1996) or Chemenda et al. (1997), it must be strongly emphasized that the exhumation process is not only controlled by

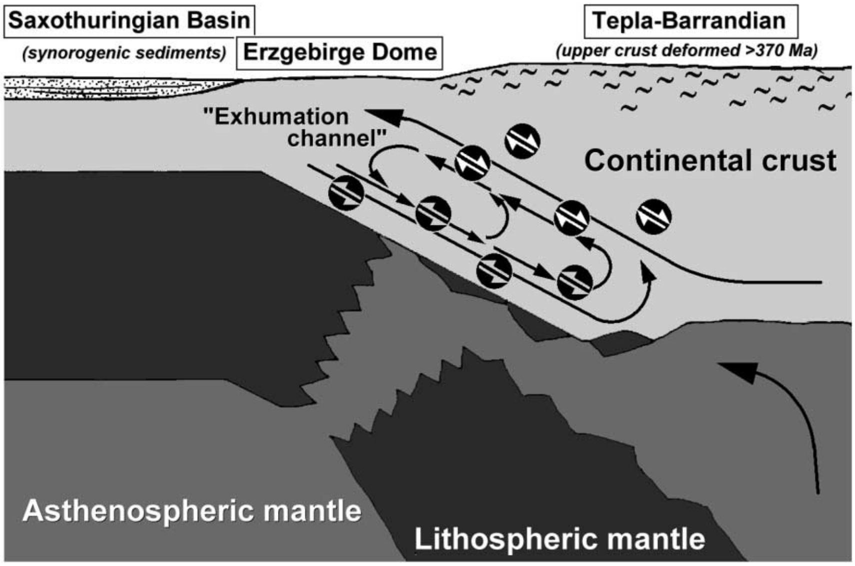

Fig. 3. General conceptual scenario for the exhumation of rocks from the crustal root in the northern part of the Bohemian Massif immediately after delamination of the lithospheric mantle. The extrusion process caused large-scale forced convection within the crust. Units undergoing orogen-parallel extension at intermediate to upper-crustal levels are contemporaneously underthrust by units undergoing prograde metamorphism and compressional deformations.

discrete narrow tectonic zones, but by penetrative internal deformation affecting the *whole volume* of exhuming rocks. The model suggests that hot lower crust rising up against cooler upper crust and concomitantly subducting cool upper-crustal rocks proceeded as consequence of secondary-forces convection (e.g. Schott and Schmeling, 1998). The result is documented in the Erzgebirge as a complicated pile of tectonometamorphic units of very different size that were juxtaposed at very different depths. Strong differences in peak metamorphic P–T conditions are recorded in adjacent rock types (e.g. Willner et al., 2000). The P–T trajectories of the high- to ultra-high-pressure rocks exhumed at 340 Ma in many parts of the Bohemian Massif are mainly characterised by early near-isothermal decompression at high temperature and decompression/cooling paths from mid- to upper crustal levels (Fig. 4). However, the geometry of these isolated trajectories varies strongly from locality to locality, and hence for detailed modelling the interrelated set of PTtd-paths derived in the Erzgebirge dome are preferred for the present study. The extensional features imprinted during the Upper Carboniferous that dominate the overall structure of the Bohemian Massif are described in detail by Krohe (1998).

Franke and Stein (2001) recently proposed an alternative exhumation model for high-grade rocks along the northern Bohemian Massif. The PTtd-relationships that we consider to be of paramount importance for delineating the sequence of geodynamic events do not play a prominent role in their analysis. This model also concludes that high-grade rocks are exhumed by extrusion within a low viscosity zone, but no detachment of the lithospheric mantle is assumed as a driving force for this geologically very abrupt phenonemon. The general scenario is patterned after geodynamic models proposed by Chemenda et al. (1997). Stacking of rock sequences is assumed to proceed during exhumation, a conclusion in line with traditional ideas of foreland-directed

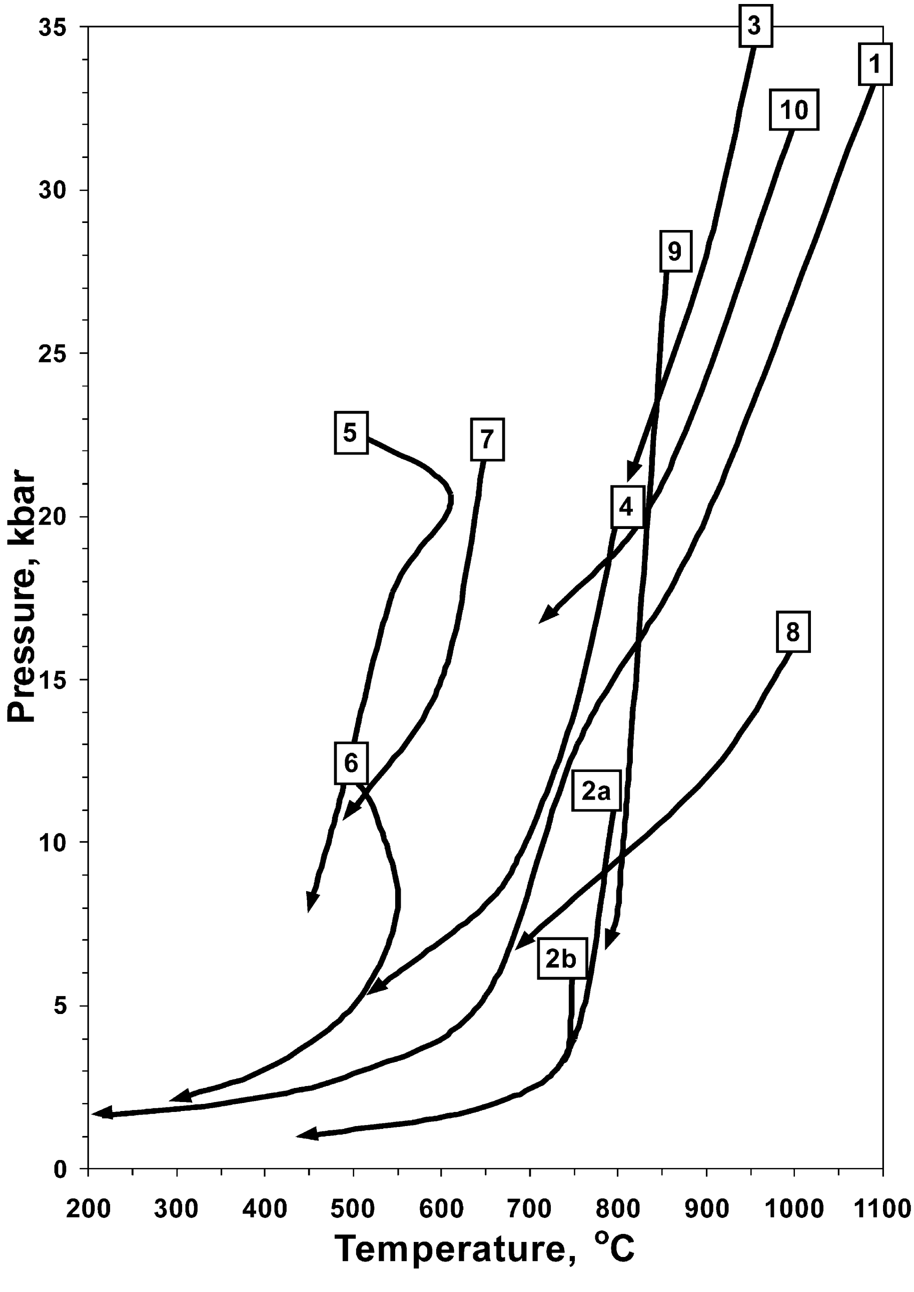

Fig. 4. Summary of P–T trajectories related to exhumation of metamorphic rocks in the Bohemian Massif at ~340 Ma. Numbers refer to the following regions and authors: 1—Lower Austria (garnet peridotite; Carswell, 1991); 2—Granulitgebirge [(a) acid granulite, (b) cordierite-garnet gneiss; Reinhardt and Kleemann, 1994]; 3—Central Erzgebirge (diamondiferous gneiss; Massonne, 1999); 4—Central Erzgebirge (acid granulite; Willner et al., 1997b); 5—Central Erzgebirge (eclogite; Massonne, 1992); 6—Western Erzgebirge (mica schists; Rötzler et al., 1998); 7—Western Erzgebirge (eclogite; Schmädicke et al., 1992); 8—Lower Austria (acid granulite; Carswell and O'Brien, 1993); 9—Southern Bohemia (garnet-orthopyroxene fels; Kotková et al., 1997); 10—Snieznik/Polish Sudetes (acid granulite; Kryza et al., 1996).

thrusting. However, it has been pointed out that such thrusting is not compatible with the kinematic pattern observed in the Erzgebirge region (Fig. 2; see discussion in Krohe, 1998).

3. Interrelated P–T-deformation-time paths of the Erzgebirge dome—petrological evidence for the exhumation history

The rocks of the Erzgebirge dome at the northern margin of the Bohemian Massif provide detailed evidence for mechanisms of very rapid exhumation of rock slices from extreme crustal depths. The dome has an onion-like antiformal structure (Fig. 2) consisting of subhorizontal composite tectonometamorphic units from different levels of the thickened Variscan crustal bulge. This presently exposed crustal profile has been extremely reduced by ~90% to a thickness of about 5–6 km through tectonic processes active during the exhumation caused by extension of a crustal bulge at ~340 Ma (Krohe, 1998; Willner et al., 2000). Intrusion of huge post-tectonic granite plutons around 324–305 Ma into an uppermost crustal level and a regional unconformity around 326 Ma complete the exhumation history.

Five tectonometamorphic units are distinguished from structural top to bottom (Fig. 2), namely the *phyllite unit*, the *garnet-phyllite unit,* the *mica-schist/eclogite unit,* the *gneiss/eclogite unit* and the *red-and-grey-gneiss unit*. These units represent nappe-like entities characterized by composite rock associations that are, however, internally incoherent with respect to the maximum pressures reached (Willner et al., 2000). Nevertheless, they reveal common overall trends in their metamorphic evolution and specific exhumation P–T paths (Fig. 5, for a detailed review see Willner et al., 2000).

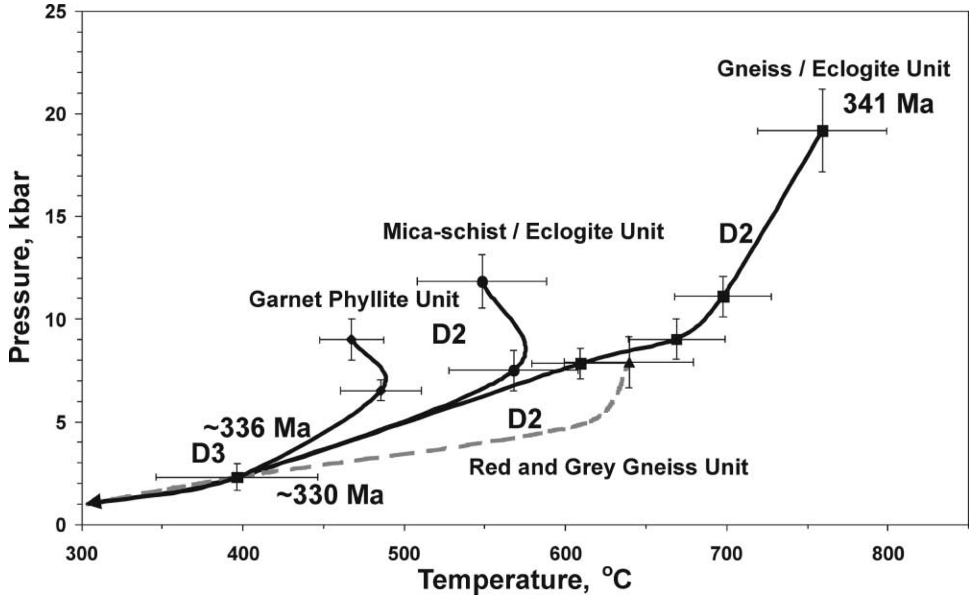

Fig. 5. Summary of interrelated P–T-time-deformation paths for the exhumation of the tectonometamorphic units of the Erzgebirge (for details see Willner et al., 2000). Data are given only for the quartzo-feldspathic and pelitic rocks constituting the bulk volume of each unit.

The *phyllite unit* (*PU*) overlying the Erzgebirge dome in the NW and W contains the only biostratigraphically dated metasediments (Cambrian to Lower Devonian), and may be correlated with those of the adjacent syntectonically subsiding Saxothuringian basin. The lowest maximum P–T conditions (2 kbar / 300 °C; Willner et al., 2000) are encountered here. Structurally below this, two units are exposed which have similar P–T paths, but differ in maximum P–T conditions (Rötzler et al., 1998) that increase from the structurally higher *garnet-phyllite unit* (GPU; 9 kbar/470 °C) to the underlying *mica-schist/eclogite unit* (*MEU*, 12 kbar/550 °C). The quartzo-feldspathic and pelitic rocks of the MEU and the GPU were slightly heated up to ~50 °C during exhumation to a mid-crustal level (6–8 kbar; "decompression/heating path"). This led to a convergence with the P–T path of the underlying gneiss/eclogite unit. At the same time, penetrative non-coaxial deformation (D_2) occurred, mainly with a top-to-W sense of shear. With continuing exhumation and cooling, discrete ductile normal faults with a similar sense of shear originated (D_3). White mica Ar–Ar ages (Werner and Lippolt, 2000) indicate that the mica-schist/eclogite and underlying gneiss/eclogite units were brought together and exhumed to a shallow crustal level between 340 and 330 Ma.

The *gneiss/eclogite unit* (GEU) contains the rocks with the highest maximum P–T conditions: 21 kbar/830 °C are recorded in the quartzo-feldspathic rocks constituting the bulk of the unit (Willner et al., 1997b). Intercalated small bodies of high-temperature eclogites and garnet peridotites commonly indicate much higher maximum pressure conditions well within the coesite stability field (Massonne, 2001). Moreover, microdiamonds have recently been found in two quartzo-feldspathic lenses (Massonne, 1999; Stöckhert et al., 2001) indicating peak metamorphic conditions up to 45 kbar (minimum pressure) and 950 °C. The quartzo-feldspathic rocks display a typical "decompression/cooling path" and a strong penetrative deformational imprint *post-dating* crustal stacking. The resulting dominant foliation (D_2) represents strong ductile thinning by stretching and was generally overprinted at 6–8 kbar by recrystallisation and static mineral growth brought about by an external fluid influx, presumably due to underthrusting by a cooler plate undergoing prograde dehydration (Willner et al., 2000). During further exhumation and cooling, discrete ductile normal faults originated again at a 2–3 kbar level (D_3). Lenses of medium-pressure/low-temperature rocks exhibiting relic prograde deformational structures were incorporated at this stage. Multifacetted metamorphic zircons, which grew at high pressures (as indicated by phengite inclusions) and before the thermal peak of metamorphism, have an age of 341 Ma (Pb–Pb-evaporation method; Kröner and Willner, 1998) and thus date the high-pressure event. Ar–Ar cooling ages of white mica around 340 Ma (Werner and Lippolt, 2000) point to initial exhumation rates in excess of 10 mm/a and cooling rates in excess of 50 °C/km. Some rocks at the base of the gneiss/eclogite unit must have been reheated, as indicated by resetting of Ar–Ar-ages around 330 Ma (Werner and Lippolt, 2000).

The *red-and-grey-gneiss unit* (RGGU) is the lowermost tectonometamorphic unit of the Erzgebirge dome. It mainly consists of orthogneisses that were predominantly exhumed from a mid-crustal level (6–8 kbar; 600–700 °C; Willner et al., 1995; Klemm, 1995). This obvious metamorphic inversion suggests that the RGGU was thrust under the overlying gneiss/eclogite unit during its exhumation. Penetrative non-coaxial deformation, however, occurred at shallow crustal depths (2–4 kbar) and at temperatures above 500 °C. Thus diverging shear zones (D_2) with "top-to-W, top-to-NW and top-to-SE" transport led to the final formation of the Erzgebirge dome structure. Ar–Ar and Rb–Sr ages of synkinematic white micas around 330 Ma (Tichomirova et al., 1996; Werner et al.,

1997) date the formation of this structure, at which time the overlying units had already been cooled. Again, younger discrete ductile normal faults formed during the subsequent cooling and exhumation path (D_3). The lowermost exposed levels of the RGGU are characterized by a high-temperature/low-pressure overprint well inside the sillimanite stability field, which is distinctly different from the overlying units. This also represents a late increase of the geothermal gradient.

Deformation related to exhumation of the tectonometamorphic units is regarded as mainly extensional, while compressional structures related to the prograde (subduction) stage are found as relic structures only or may be proved by relic metamorphic inversions (Willner et al., 1995, 2000). It also appears that exhumation of the high pressure rocks from the crustal root occurred in approximately the same zones (Fig. 3) of the orogenic belt where these rocks had originally been subducted to great, partly even to mantle depths (Willner et al., 2000). During this exhumation process, Lower Carboniferous greywackes were deposited into the neighbouring Saxothuringian basin. This required considerable submarine relief, but not necessarily a major topographic expression.

The exhumation of high-pressure rocks in the Erzgebirge was coeval with the emplacement of similar ultra-high-, high-, and medium-pressure rock associations around 340 Ma in many parts of the Central European basement (cf. Kröner and Willner, 1998, for summary).

4. Two-dimensional numerical modelling of the exhumation of crustal rocks

4.1. Method

To model the exhumation of metamorphic rocks after lithospheric delamination and detachment we followed the dynamically, rheologically and thermally consistent modelling procedure (FDCON) established, programmed and tested by Schmeling (1989), Schmeling and Bussod (1996), Schott and Schmeling (1998). In this fluid-dynamic convection approach, the equations of conservation of energy, momentum and mass are solved on an equidistant grid by the method of finite differences. Since the modelling procedure, tests and examples are discussed in great detail in several publications (e.g. Schmeling, 1989; Schmeling and Bussod, 1996; Schott and Schmeling, 1998; Schott et al., 2000) only a short summary is given below.

4.2. Basic equations

The following differential equations were used for heat-conducting viscous flow in the gravitational field (e.g. Schott and Schmeling, 1998; Schott et al., 2000). Conditions for the conservation of mass and momentum were combined in the dimensionless biharmonic equation for the stream function ψ (e.g. Schott and Schmeling, 1998; Schott et al., 2000)

$$\left(\frac{\partial^2}{\partial z^2}-\frac{\partial^2}{\partial x^2}\right)\eta\left(\frac{\partial^2\psi}{\partial z^2}-\frac{\partial^2\psi}{\partial x^2}\right)+4\frac{\partial^2}{\partial x\partial z}\eta\frac{\partial^2\psi}{\partial x\partial z}=-Ra\frac{\partial T}{\partial x}-Rc\frac{\partial C}{\partial x} \tag{1}$$

where $Ra = r_o g\alpha\Delta Th^3/\kappa\eta_o$ and $Rc = \Delta\rho gh^3/\kappa\eta_o$ are thermal and chemical Rayleigh numbers, respectively; x and z are horizontal and vertical coordinates; C is the chemical field (composition function); T is temperature; g is the acceleration within the gravity field; $\eta_o = 10^{21}$ Pa·s is the scaling viscosity ; h is the distance between the bottom and the top of the model; ρ_o is the reference density; $\Delta\rho$ is the density difference due to the chemical composition; α is the thermal expansivity.

The dimensionless equation for the heat transport is

$$\frac{\partial T}{\partial t} + (v \cdot \nabla)T = \nabla \cdot (\kappa \nabla T) + H + Di\left(\frac{\Phi}{Ra} - v_z T\right) \tag{2}$$

where $v_x = \partial\psi/\partial z$ and $v_z = -\partial\psi/\partial x$ are components of the velocity vector v; $Di = \alpha g h / C_p$ is the dissipation number; H is the internal heat production; $\Phi = 2\eta\epsilon_{ij}\epsilon_{ij}$ is the dissipation function with $\epsilon_{ij} = \frac{1}{2}(\partial v_i/\partial x_j + \partial v_j/\partial x_i)$ being an element of the strain-rate tensor; κ is the thermal diffusivity; C_p is the isobaric heat capacity.

The viscosity η was determined via a rheological equation. For the upper and lower crust a constant viscosity of 10^{23} Pa*s and 10^{20} Pa*s (Schott and Schmeling, 1998) was used respectively. The mantle (lithosphere and asthenosphere) rheology was represented by temperature- and pressure-dependent dislocation creep with a power-law exponent of 3.5 and superimposed two creep laws (Schmeling and Bussod, 1996; Schott and Schmeling, 1998; Schott et al., 2000)

$$\varepsilon_{\text{tot}} = \varepsilon_1 + \varepsilon_2 = 10^{-17}\Delta\sigma^{3.5}\left(2.1P_{O_2}^{0.02} + 52P_{O_2}^{0.23}\right)\exp\left(-\frac{540000 + 0.000015P}{8.314T}\right), \tag{3}$$

$$\log_{10}\left(P_{O_2}\right) = 9 - \frac{25738}{T} + 0.092\frac{P-1}{T},$$

where $\Delta\sigma$ is the difference between the maximum and the minimum stress, Pa; P is pressure, atm; P_{O_2} is partial pressure of oxygen, atm. The viscosity was truncated with an upper limit of $\eta_{\max} = 10^{25}$ Pa*s and a lower limit of $\eta_{\min} = 10^{18}$ Pa*s.

4.3. Numerical solution

The fourth-order equation for the stream function [Eq. (1)] was solved by a direct method using a finite-difference technique on an equidistant grid in a rectangular box of aspect ratio 2, and a resolution of 61x121 points in the z- and x-direction respectively. The heat transfer equation [Eq. (2)] was solved by an ADI-scheme, but with a resolution four times larger. A marker technique was employed for the advection of the different components. Marker points containing material property information were initially distributed on a regular rectangular (marker) grid. The markers were moved through the mesh according to the calculated velocity field. In numerical experiments between 1.8×10^5 and 1.5×10^6 markers were used, depending on the desired resolution. For a detailed technical description on the method of solution see Schmeling and Marquart (1991). The accuracy of the code has been ascertained in several benchmark tests (Blankenbach et al., 1989; van Keken et al., 1997).

4.4. Modelling of P–T paths

The program procedure employed allowed a P–T path to be modelled for each given marker by using calculated temperature fields at each t = constant, with pressure represented as a function of depth and density of the rocks. This allowed the investigation of the shape of a path and the distribution of numerous P–T paths in the modeled sequence. The comparison of such theoretically derived P–T paths with those obtained from mineral geothermobarometry represents, in addition to geometry, an important constraint on possible geodynamic regimes of metamorphic complexes. The evolution of the thermal field and the shape of the modelled P–T paths depend mainly on the relationship between convective and conductive heat flows. Taking into account the relatively small variations in ρ, κ and c_p of the rocks involved, this relationship is mainly defined by velocity fields and, thus, by the timescale of the geodynamic processes modelled. Therefore the consistency between the shapes of geothermobarometric and modelled P–T paths can be used to monitor the correct timing of different stages in the evolution of the modelled complexes during numerical experiments (Gerya et al., 2000).

4.5. Specific model design

In our model design (Fig. 6, Table 1) we generally followed the model geometry as well as initial and boundary conditions employed by Schott and Schmeling (1998) and Schott et al. (2000) for their generalized study of the dynamics of delamination and detachment of a lithospheric root. Schott and Schmeling (1998) examined the physical parameter range for this numerical model and found three different regimes of behaviour of the orogenic root of the mantle lithosphere: no delamination, delamination only and delamination with complete detachment. For a fixed viscosity of the upper crust of 10^{23} Pa*s delamination occurs for a range of viscosities of 10^{23} to 10^{20} Pa*s for the lower crust, depending on the thickness of the lithospheric root. However, full detachment of the delaminated lithospheric slab only occurs if the viscosity of the lower crust is greater than 10^{21} Pa*s. Lithospheric roots with a minimum vertical extent of at least 100–170 km are needed to provide sufficient negative buoyancy to allow delamination and detachment.

We used the results of Schott and Schmeling (1998) to design the geometry of our own numerical experiments (Fig. 6, Tables 1 and 2), that is to simulate the *delamination and complete detachment regime*. However, in their study these authors were not concerned with the geodynamic details of crustal processes *after* detachment. In order to provide the necessary boundary conditions at the beginning of our experiment several arbitrary assumptions had to be made to induce rapid slab detachment and to impose a realistic initial geothermal gradient in the crust at the beginning of the experiment. We proceeded with a two-layered crust and a lithospheric mantle thickened by factors of 3.8–4.0 for the compositional variation and 1.2–2.0 for the thermal structure as starting conditions (Fig. 6), in order to approach the PT conditions deduced for the Erzgebirge dome and other HP units of the Bohemian Massif at peak pressure conditions (Figs. 4 and 5). Although this arbitrary approach for reproducing the initial geothermal gradient leads to an initial maximum crustal thickness exceeding the actual value of 70 km, this assumption has no influence on the further development of the model. Taking into account the possible complexity of the internal structure of the crustal bulge created by the Variscan orogeny, which must be viewed as a tectonic collage of rock slices of different origin and multilayered detachment zones (Krohe, 1998; Willner et al.,

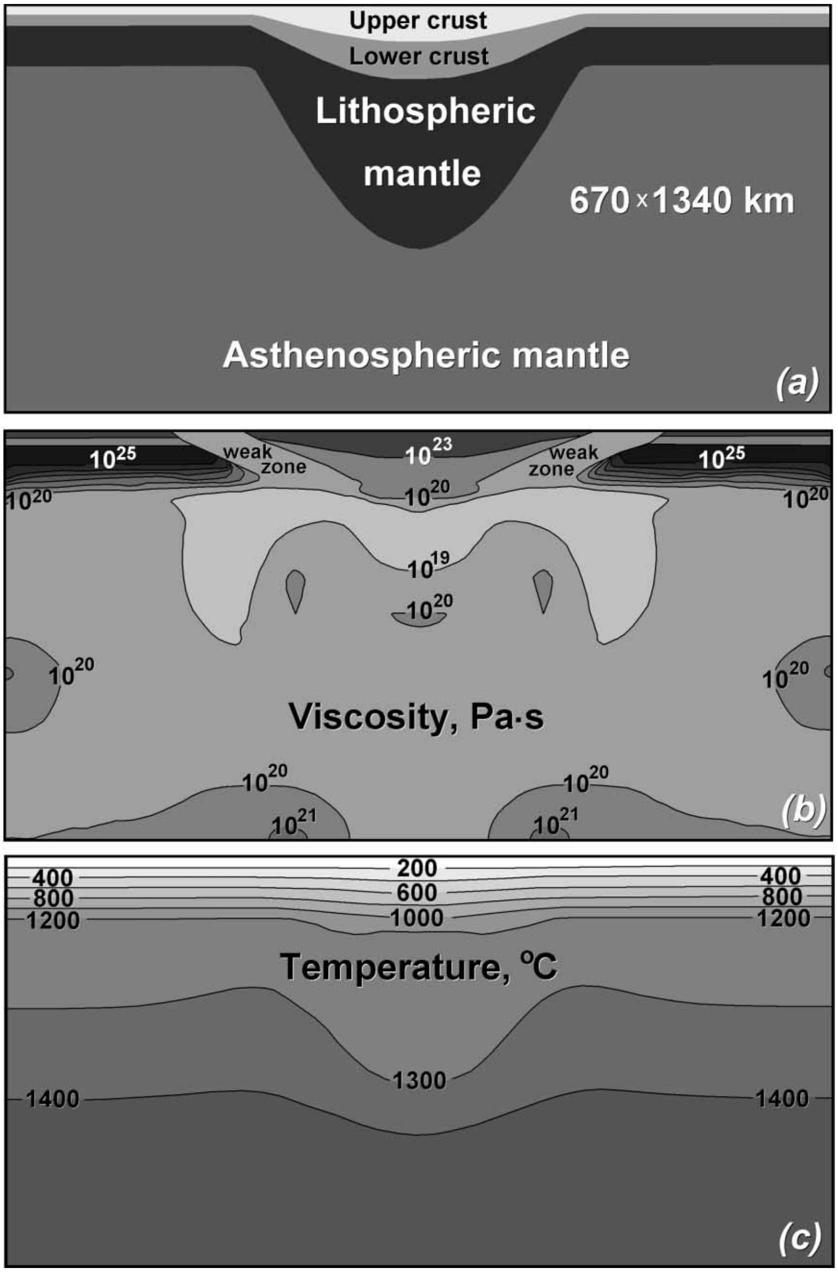

Fig. 6. Initial density (a), viscosity (b) and temperature (c) structure of the 2D numerical models studied (cf. Tables 1 and 2). See text for justification.

2000), the use of a simple two-layered crust in our model reflects mineralogical (e.g. Bousquet et al., 1997) rather than lithological differences between upper and lower crustal levels.

An important simplification of our model in comparison with those of Schott and Schmeling (1998) is the use of a constant 3–5% density contrast (e.g. Bird, 1978; Pysklywec et al., 2000)

Table 1
Parameters of 2D numerical models

Boundary conditions	
Top	$T=273$ K, $\partial v_x/\partial z=0$, $v_z=0$
Bottom	$q=20.10^{-3}$ W m^{-2}, $v_x=0$, $v_z=0$
Walls	$\partial T/\partial x=0$, $\partial v_z/\partial x=0$, $v_x=0$
Density, kg m^{-3}	
Upper crust	2700
Lower crust	2900
Lithospheric mantle	3399–3465
Asthenospheric mantle	3300
Viscosity, Pa s	
Upper crust	10^{23}
Lower crust	10^{20}
Mantle (lithospheric and astenospheric)	10^{18}–10^{25}, olivine creep[a]
Weak zones	10^{20}–10^{21} Pa s
Heat conductivity, W m^{-1}K^{-1}	
Upper crust	2.00
Lower crust	1.50
Mantle (lithospheric and astenospheric)	Depth dependent[a]
at 80 km	2.87
at 100 km	3.40
at 400 km	3.80
at 670 km	4.00
Heat production, W kg^{-1}	
Crust (upper and lower)	Depth dependent[b]
Mantle (lithospheric and asthenospheric)	$6.6.10^{-12}$
Isobaric heat capacity, J kg^{-1}K^{-1}	
Crust (upper and lower)	1300
Mantle (lithospheric and asthenospheric)	1300

[a] Taken from Schmeling and Bussod (1996).
[b] $H=H_o\exp(-z/d)$, where $d=40{,}000$ m is characteristic depth and $H_o=2.7\cdot10^{-10}$ W kg^{-1} corresponds to surface heat flow $30\cdot10^{-3}$ W m^{-2} (Schmeling and Bussod, 1996).

Table 2
Summary of tested 2D models

Model	Factor of thickening of the lithosphere	Reduction of ∂T/∂z within the thickened lithosphere	Density of the lithosphere, kg m^{-3}	Width of weak zones, km	Viscosity of weak zones, Pa s
A	4.0 x	2.0 x	3465	90	10^{21}
B	4.0 x	1.2 x	3399	200	10^{21}
C	3.8 x	1.2 x	3399	150	10^{20}
D	4.0 x	1.2 x	3399	150	10^{21}

between the lithospheric and the asthenospheric mantle. This simplification is acceptable when considering the fast advection of the lithosphere when delamination and complete detachment occurs (Schott and Schmeling, 1998). Though not necessarily realistic, this assumption is necessary in order to reproduce the starting conditions for crustal exhumation, which is the aim of our study.

A further difference to the model designs by Schott and Schmeling (1998) is the introduction of a symmetric V-like system of weak tectonic low-viscosity zones existing before delamination and cutting through the entire lithosphere (Fig. 6b). In this assumption, we followed the conceptual models of Willner et al. (2000) and Zulauf (1997), which suggest a V-like shape of the system of major tectonic zones of mobility in the Bohemian Massif, where 340 Ma high pressure rocks are concentrated in both the northern and the southern part (Fig. 1). This is also consistent with mechanical experiments by Beaumont et al. (1996), who modelled the distribution of major compressional shear zones within collisional orogens. We chose the width of the zones and the density contrast between lithosphere and asthenosphere as variable parameters of the model (Table 2) to consider an effect on the exhumation of crustal rocks.

4.6. Results of the numerical models: changing geometries and mass movement

Four different models (Table 2, Figs. 7–11) were studied using the above approach. Although they differ in several important details, the same major sequence of geodynamic events related to

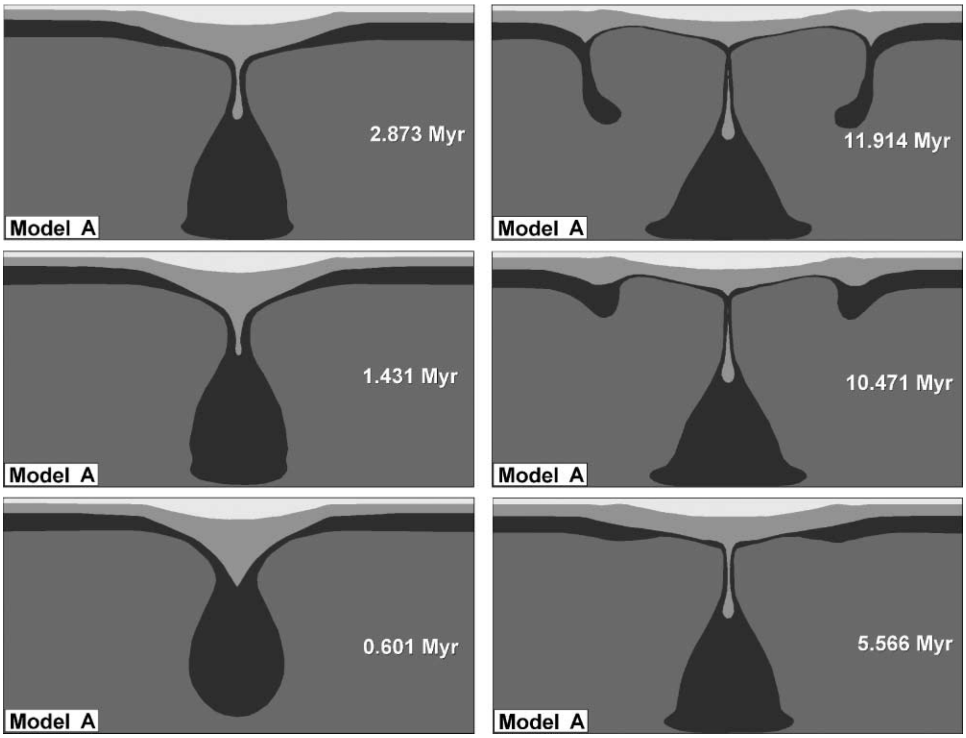

Fig. 7. Progressive lithospheric delamination and detachment for Model A (cf. Table 2). Definition of grey scales as in Fig. 6a.

the delamination and complete detachment of the lithospheric root (Schott and Schmeling, 1998) is observed. Thickening of the crust before and during detachment (e.g. Fig. 7) is followed by extension of the crust during upwelling of hot asthenosphere after detachment (Figs. 7–11). The latest stage of crustal dynamics is characterized by intense development of forced flow (Schott and Schmeling, 1998) within weak tectonic zones (Figs. 10, 11), producing "exhumation channels" for lower crustal rocks. The simulations very closely model important aspects of the lower crustal exhumation scenario of the Bohemian Massif in general and of the Erzgebirge in particular (Fig. 3; Willner et al., 2000). Hence the most important constraints to be tested were the rapid exhumation from the crustal root to the surface within a few Myr, as well as the geometry of specific PT-paths and the former "exhumation channels" within the crust.

Model A (Fig. 7). A particular feature of this model is the highest density contrast between lithosphere and asthenosphere (Table 2) during the early stage of the delamination process within the first 2 Myr. Due to the sinking lithospheric root, lower crustal material is dragged down, forming a crustal wedge penetrating to very great depths of about 250 km (Fig. 7, 0.601 Myr). The formation of a similar wedge, existing for only a few Myr before the full detachment of the lithosphere, was also observed in the numerical experiments of Schott and Schmeling (1998, Fig. 12). After detachment, a significant amount of the material of this deep crustal wedge is subducted together with the sinking lithosphere (Fig. 7, 1.431–2.873 Myr, see also Schott and Schmeling, 1998, Fig. 13). However, a part of the wedge material returns to the base of the crustal bulge (Fig. 7, 1.431–2.873 Myr) due to buoyant escape related to the high density contrast between crustal and

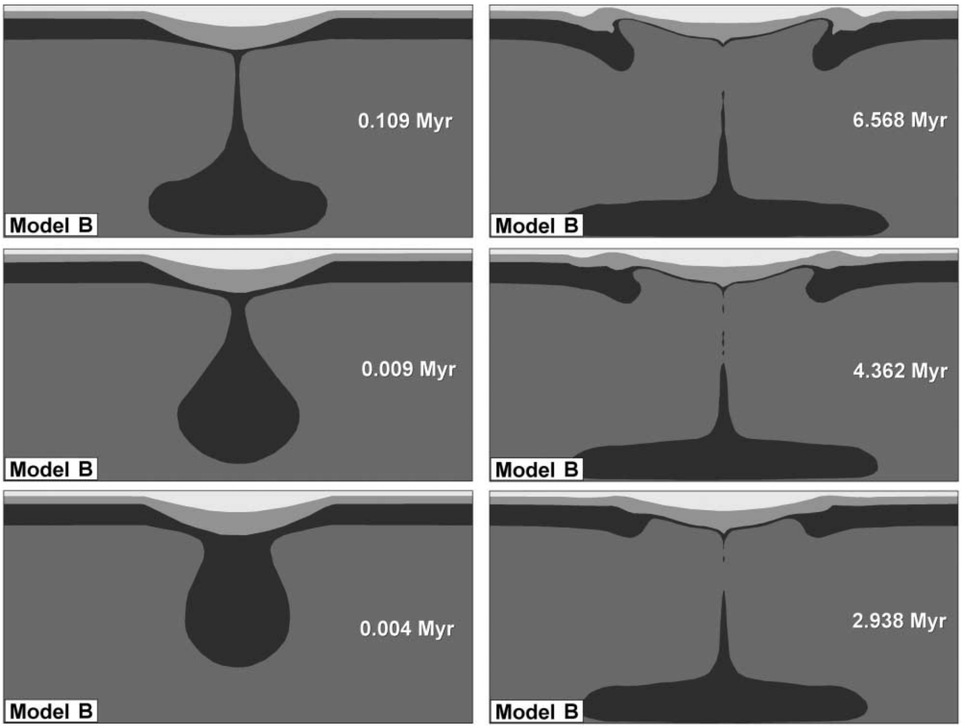

Fig. 8. Progressive lithospheric delamination and detachment for Model B (cf. Table 2). Definition of grey scales as in Fig. 6a.

mantle material. This transient, very short overthickening of the crust (formation of a deep crustal wedge) and related rapid circulation of crustal rocks at 140–200 km depth, corresponding to the diamond stability field, may explain the formation and preservation of the diamond-bearing quartzofeldspathic rocks in the Erzgebirge (Massonne, 1999; Stöckhert et al., 2001).

After about 3 Myr detachment of the lithospheric root occurs, hot asthenosphere rises to the base of the crust, and the thickened lower crust rapidly flattens out due to isostatic relaxation (Fig. 7, 2.873–10.471 Myr). Weak forced circulation of rocks within low-viscosity zones (Fig. 6) occurs at a very late stage of the process (Fig. 7, 10.471–11.914 Myr). However, no lower crustal material rises near the surface under the chosen conditions (Table 2) of minimum width and maximum viscosity of the weak zones.

Model B (Fig. 8). Doubling the width of the low-viscosity zones and decreasing the density contrast between lithosphere and asthenosphere by comparison to *Model A* (Table 2) causes significant changes in the development of the model geometry. Delamination and detachment of the lithosphere considerably accelerate to an unrealistically short time span of $\sim$0.1 Ma that could also be related to the relatively low value of $\eta_{\min} = 10^{18}$ Pa*s for the mantle material. Although initial detachment is characterized by negative (downward-directed) vertical velocities of lower crustal material (see also Fig. 12a), no significant crustal thickening occurs during delamination and no crustal material is incorporated into the mantle (Fig. 8, 0.004–0.109 Myr). Forced upward flow of lower crustal rocks within the hanging wall of the low-viscosity zones immediately starts after detachment and proceeds during the extensional crustal thinning caused by upwelling asthenosphere

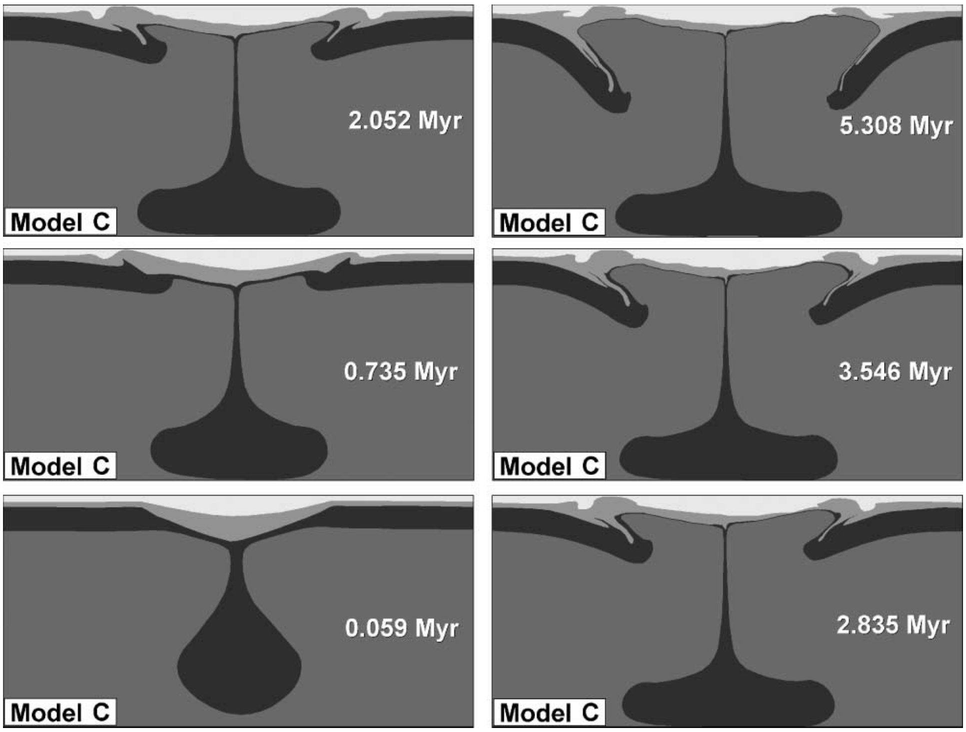

Fig. 9. Progressive lithospheric delamination and detachment for Model C (cf. Table 2). Definition of grey scales as in Fig. 6a.

(Fig. 8, 2.938–6.568 Myr). This process is accompanied by subduction of the upper crustal rocks into the footwall part of the low-viscosity zones.

Model C (Figs. 9 and 10). In comparison to *Model B,* the viscosity of the weak zones in *Model C* was lowered to $\eta_{\min} = 10^{20}$ Pa*s, corresponding to the chosen viscosity of the lower crust, and the width of the zones was decreased to 150 km (Table 2). As a result, delamination and detachment in *Model C* proceed more slowly than in Model B, i.e. within ~1 Myr. Vertical velocities of lower crustal rocks during delamination are positive (upward directed) and no additional thickening of the crust occurs at this stage. Extensional thinning of the crustal bulge proceeds very intensely and is mainly related to the removal of lower crustal rocks from the base of the thickened crust toward the weak zones (Fig. 9, 0.735–2.835 Myr, see also Koyi et al., 1999). The low viscosity of the weak zones provides intense forced flow of both the lower and upper crustal rocks within them (Fig. 10, 2.052 Myr). Exhumation of the lower crustal rocks starts relatively earlier at ~ 0.5 Myr and a near-surface level is reached within the next 1.5 Myr (Fig. 10). By comparison to *Model B* the exhumation velocity of lower crustal rocks is increased by one order of magnitude (Fig. 12), reflecting the decrease in viscosity of the weak zones. While the lower crust is intensely exhumed in the hanging wall of both low-viscosity zones and is strongly stretched between both zones, concomitant deep subduction of upper crustal material is also observed (Fig. 10, 2.052–5.308 Myr). The latest stage of development is manifested by progressive delamination of the

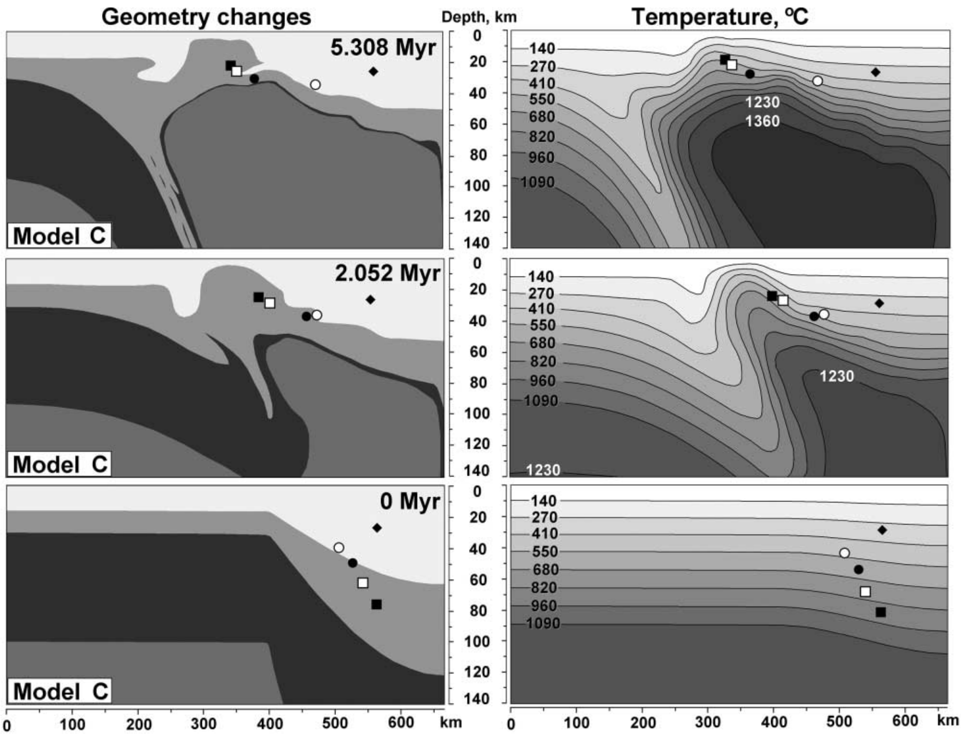

Fig. 10. The evolution of the density (left side) and temperature (right side) structures of the crust and upper mantle in Model C (Table 2). Separate sketches represent 670×140 km sections of Model C (Fig. 8). Markers show displacement of specific fragments of upper and lower crust.

lithosphere starting from the area of the previously existing lithospheric bulge (Fig. 9, 2.052–5.308 Myr). A similar process was theoretically studied by Bird (1978) assuming an 83 kg/m^3 density contrast between lithosphere and asthenosphere. A significant amount of lower crustal rocks is stacked with the lithospheric mantle and progressively subducted to great depth during this process (Fig. 9, 2.052–5.308 Myr). The stacking of lower- and upper-crustal rocks within weak zones also occurs at this stage (Fig. 10, 5.308 Myr).

Model D (Fig. 11). This model differs from *Model C* only in the higher viscosity of the weak zones (Table 2). As a consequence, the development of forced flow within the weak zones and the removal of material from the base of the overthickened crust are clearly less intense (compare Figs. 10 and 11).

4.7. Results of the numerical models: P–T-time paths for the exhumation of crustal rocks

Despite significant differences in the details of lithospheric detachment and associated crustal dynamics (Figs. 7–11), all models studied demonstrate similar general features in terms of characteristic physical trajectories and P–T-time paths of exhuming rocks (Figs. 12–16). The highest exhumation velocities (Fig. 12) and the most significant horizontal and vertical displacements (Figs. 10, 13a and b and 14a and b) are observed for rocks of the lower crust characterized by a low effective viscosity and high mobility (e.g. Ranalli, 1995; Koyi et al., 1999). Both, the horizontal

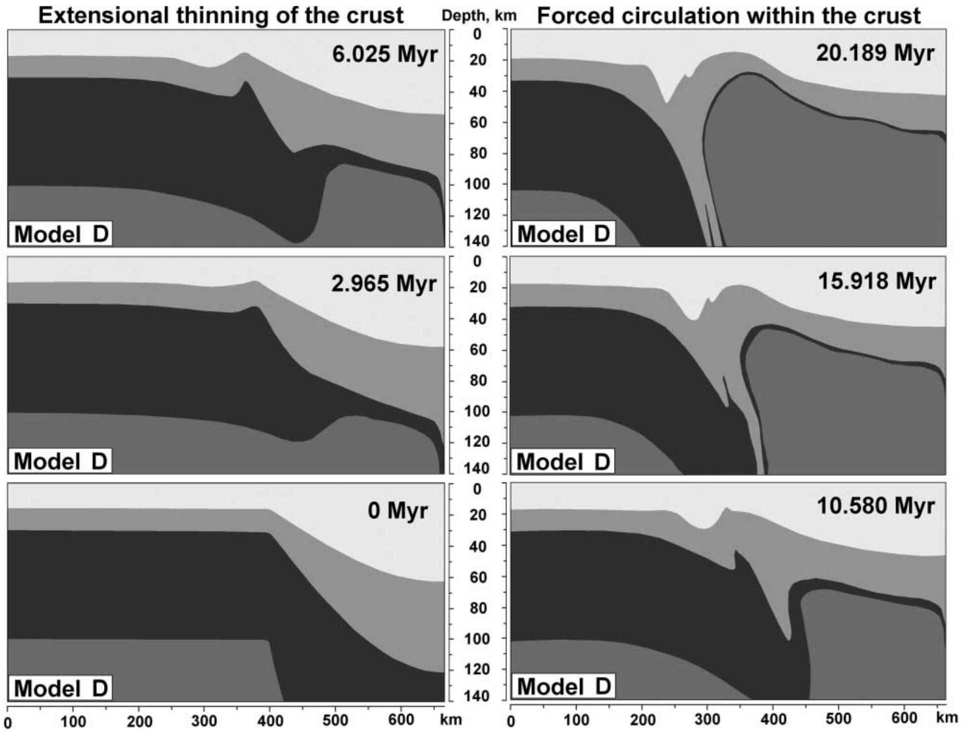

Fig. 11. Progressive lithospheric delamination and detachment for Model C (cf. Table 2). Definition of grey scales as in Fig. 6a.

and the vertical displacements show a positive correlation (Figs. 13c and 14c) with the initial depth of the rocks in the modelled sections. Most of the vertical displacement and exhumation of lower crustal rocks occur at the stage of intense extensional crustal thinning (Figs. 13b and 14 b). This exhumation is also associated with very strong (up to 150–200 km) horizontal displacement of lower crustal rocks from the base of the thickened crust toward the weak zones (Figs. 13a and

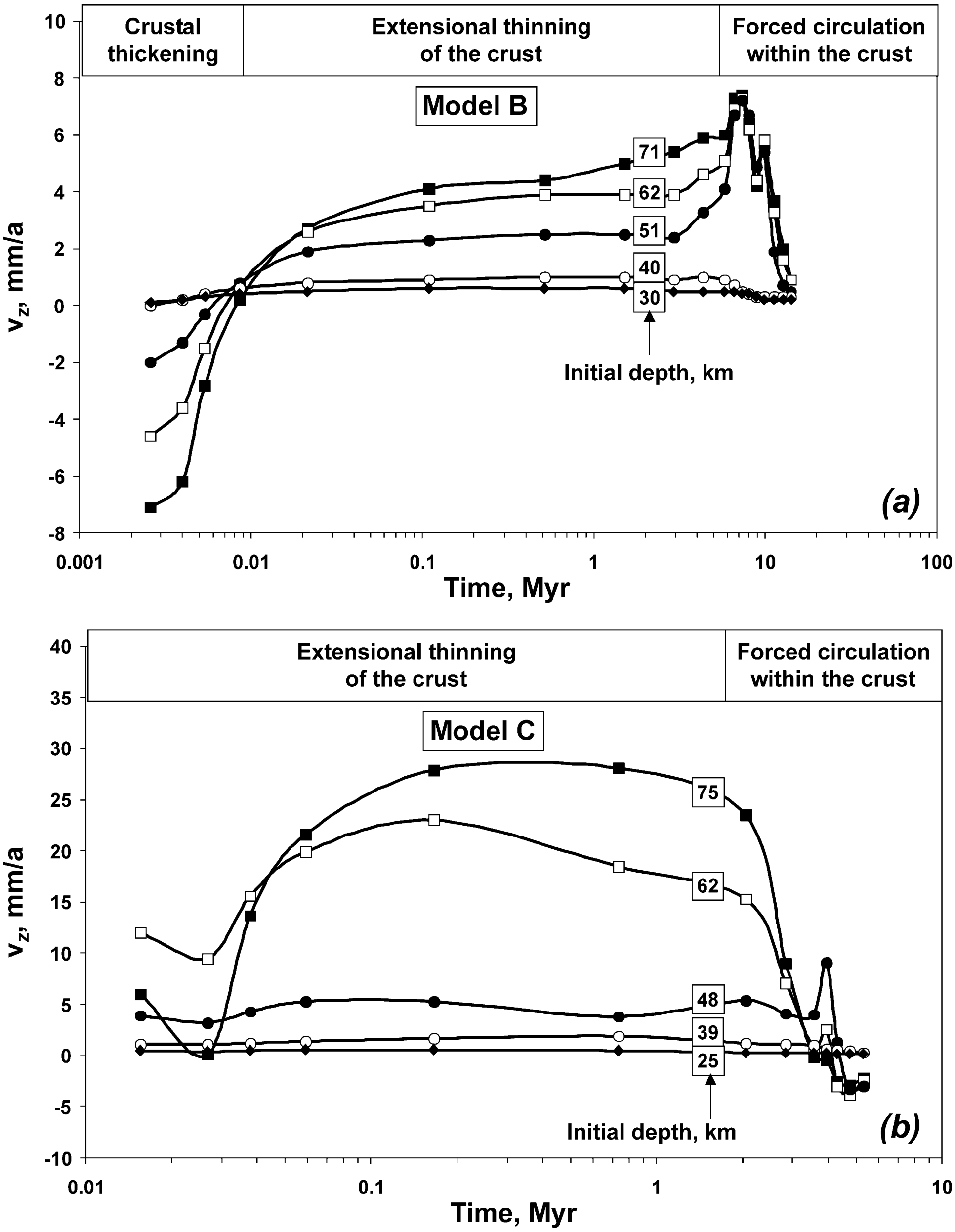

Fig. 12. Variation of vertical (exhumation) velocity with time for the markers from different crustal levels (Fig. 10) in Models B (Table 2, Fig. 8) (a) and C (Table 2, Fig. 10) (b).

14a), producing a strong inversion in the initial position of different crustal fragments (Fig. 10). The later stages of exhumation are clearly associated with extensional deformation in a middle-upper crustal level (Fig. 10, 2.052–5.308 Myr), an observation that is consistent with geological data from the Bohemian Massif and, particularly, from the Erzgebirge Dome.

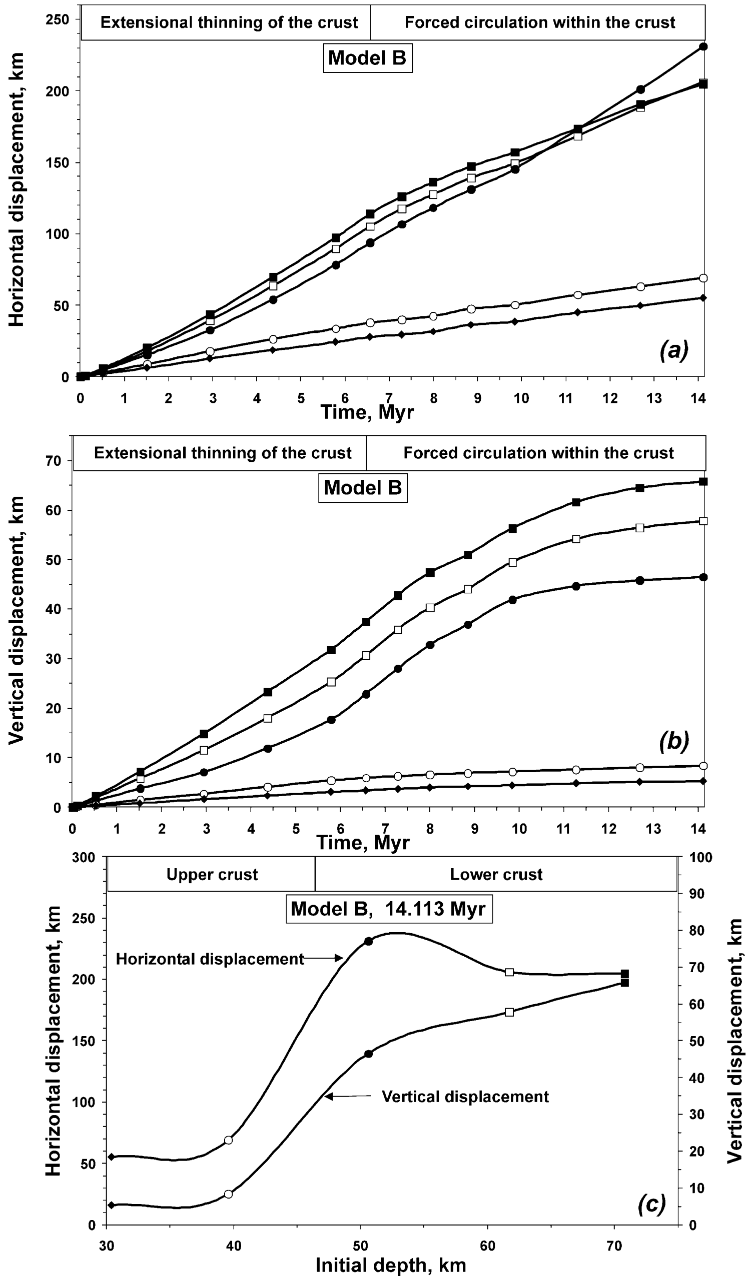

Fig. 13. Horizontal displacement vs. time (a), vertical displacement vs. time (b) and horizontal displacement vs. initial depth (c) relationships for markers from different crustal levels in Model B (Table 2, Fig. 8).

The modelled P–T-time trajectories are shown in Figs. 10, 15, and 16. For the lower crustal rocks the dT/dP-slopes of the decompression/ cooling trajectories decreases with time from 10–20 K/kbar at the early stage of exhumation to 40–50 K/kbar at the later stage (Figs. 15 and 16). Upper crustal rocks are characterized by relatively short P–T paths that are clearly related to the weak displacement

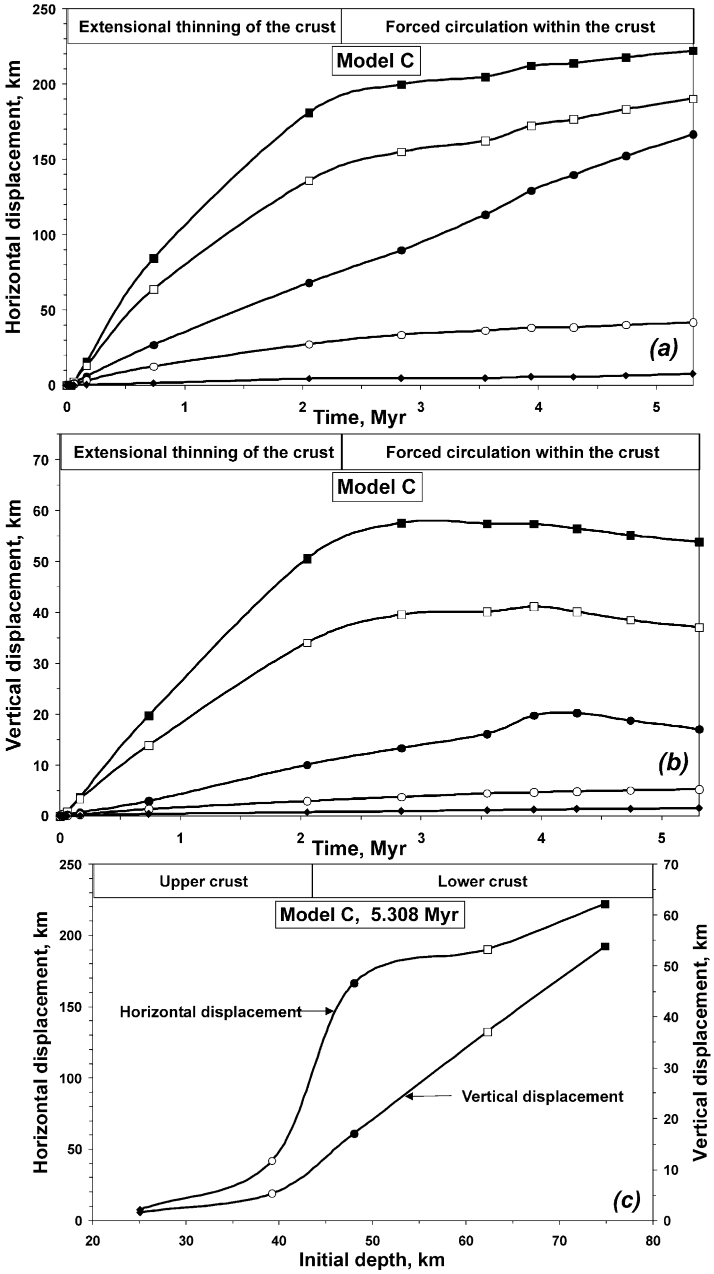

Fig. 14. Horizontal displacement vs. time (a), vertical displacement vs. time (b) and horizontal displacement vs. initial depth (c) relationships for markers from different crustal levels (Fig. 10) in Models C (Table 2, Fig. 9).

of these rocks during crustal extension (Fig. 10). During the later stages of exhumation the P–T trajectories of both lower- and upper-crustal rocks commonly demonstrate an increase in temperature at a pressure of 6–9 kbar, corresponding to the middle crustal level. This increase is caused by upwelling of the hot mantle lithosphere, underplating relatively cold crust (Fig. 10).

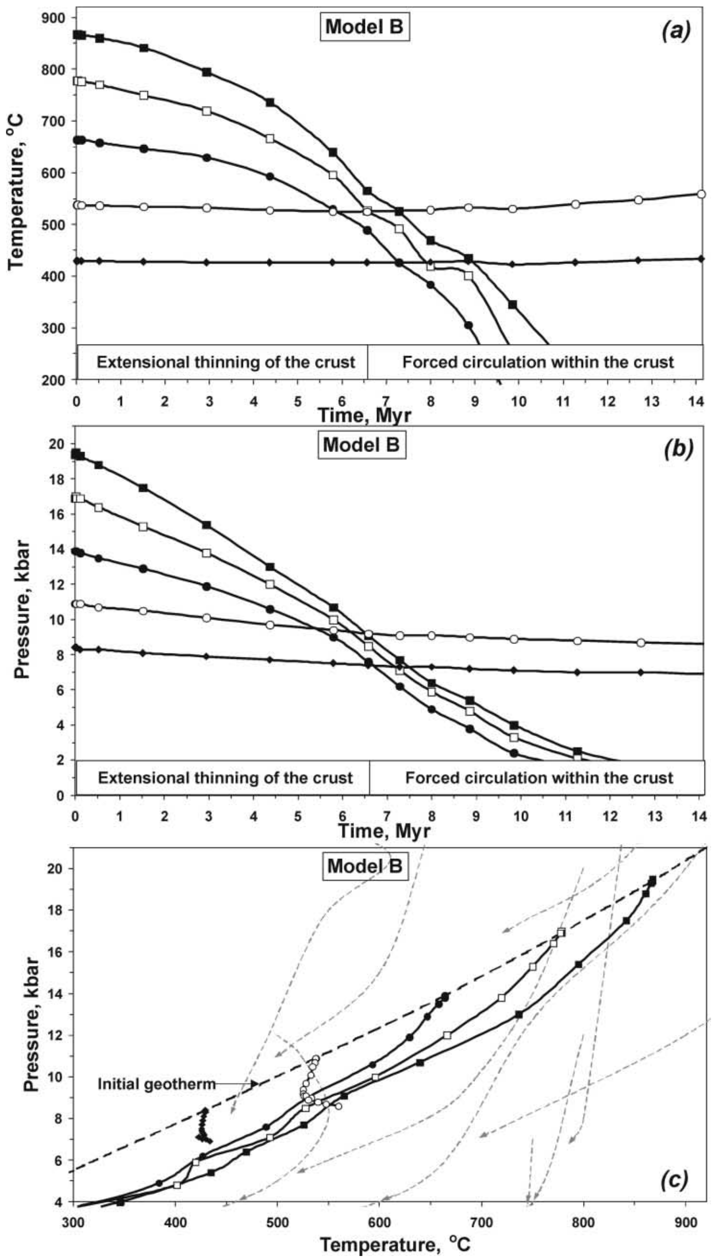

Fig. 15. Modelled P–T-time paths (solid lines) for markers from different crustal levels in Model B (Table 2, Fig. 8). Different diagrams show temperature-time (a), pressure-time (b) and P–T projections of the paths. The observed P–T trajectories of metamorphic rocks of the Bohemian massif (Fig. 4) are shown by dashed gray lines.

Although the general pattern of modelled P–T trajectories does differ from the P–T path data collected for the Bohemian Massif from the literature (Figs. 15c and 16 c), three important features of this array are indeed reproduced: (i) lower crustal rocks show decompression/cooling P–T paths, (ii) P–T paths do not follow one single uniform exhumation trajectory and (iii) both decompression/cooling and decompression/heating P–T paths are found. The diversity of the P–T paths is caused by the diversity of physical trajectories of the investigated rocks in a non-homogeneous (both in time and space) thermal field, disturbed by rapid (5–30 mm/a) movement of mantle and crustal material. Therefore, the diversity of the P–T paths of the Bohemian Massif can be interpreted as a direct consequence of the relatively short (a few Myr) time-scale of geodynamic processes affecting this area at $\sim$340 Ma. This is also consistent with the existing geochronological data described above.

Any further attempt to arrive at a closer convergence between the P–T paths derived from 2D modelling and those derived from geothermobarometric data would require more precise information on the exact geometry of the Variscan Bohemian Massif. Such data remain very speculative at present. However, the comprehensive natural P–T-deformation-time record available for the metamorphic rocks of the Erzgebirge dome (see above) is much more amenable to realistic one-dimensional thermal modelling of the exhumation process. This modelling was aimed not only at reproducing of the assemblage interrelated PTtd-paths, but also at deriving further theoretical constraints on the timing of the exhumation process. As shown by Gerya et al. (2000), converging consistency between the shapes of modelled and observed P–T paths allows estimation of the correct time-scale of the corresponding metamorphic process. The uncertainties of timing in this case are mainly defined by the uncertainty in the thermal diffusivity of rocks. Therefore, time estimates of the exhumation based on modeling of P–T paths may vary within half an order of magnitude (Gerya et al., 2000). Such data are extremely important, because the overlap of errors in the radiometric age data during this rapid event generally precludes detailed chronological resolution.

5. One-dimensional modelling of the interrelated P–T-time paths of the Erzgebirge Dome

5.1. Method

One-dimensional modelling experiments of the P–T-time paths of metamorphic rocks were performed using a procedure developed and programmed by Peacock (1989). A one-dimensional, time-dependent, heat transfer equation is solved written in the form

$$\frac{\partial T}{\partial t} = \kappa \frac{\partial^2 T}{\partial z^2} v_z \frac{\partial T}{\partial z} + \frac{H}{C_p} \tag{4}$$

where T is temperature, K; t is time, s; κ is thermal diffusivity, m^2/s; z is depth, m; v_z is velocity of the medium in z direction, m/s; H is heat production, W/kg; C_P is isobaric heat capacity, J/(kg K); ρ is density, kg/m^3.

It is clear from the two-dimensional numerical models presented above that the P–T paths of the different metamorphic units of the Erzgebirge (e.g. Figs. 10 and 16) are unlikely to represent simple vertical motion of crustal material, thus casting doubt on the validity of one-dimensional

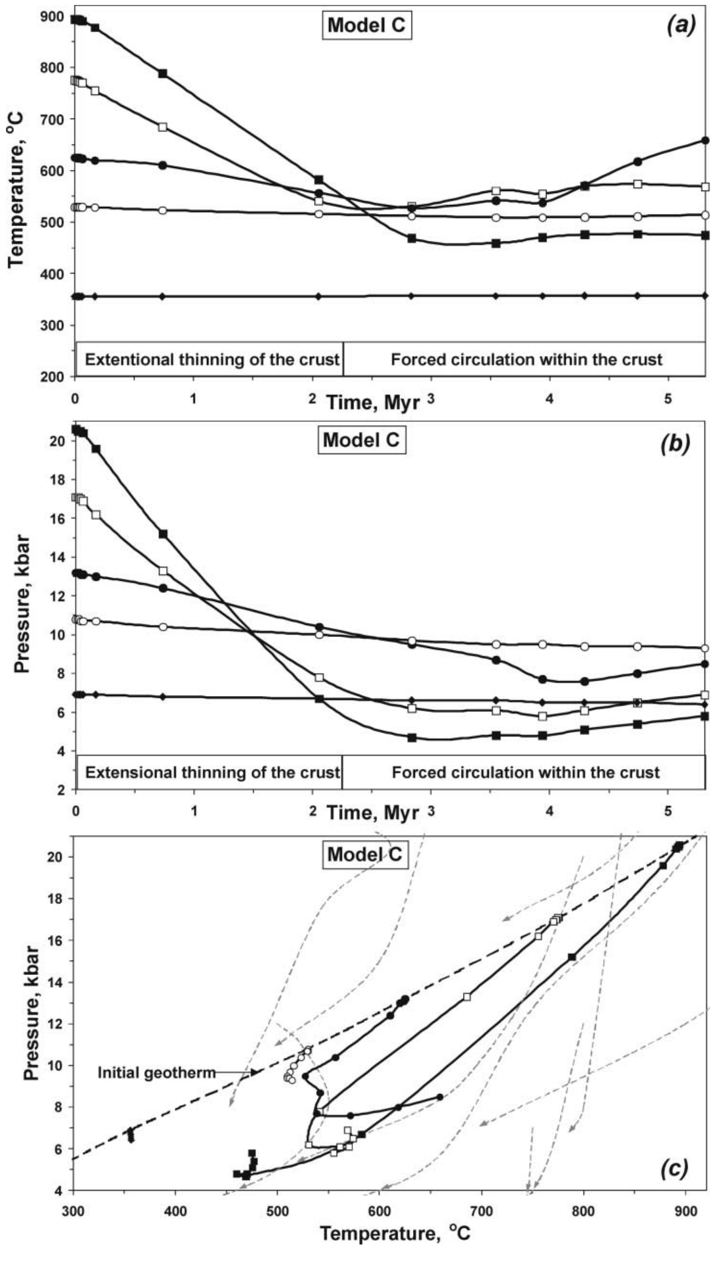

Fig. 16. Modelled P–T-time paths (solid lines) for markers from different crustal levels (Fig. 10) in Models C (Table 2, Fig. 9). Different diagrams show temperature-time (a), pressure-time (b) and P–T projections of the paths. Observed P–T trajectories of metamorphic rocks of Bohemian massif (Fig. 4) are shown by dashed gray lines.

considerations. Nevertheless, the complexity of motion of metamorphic rocks during the exhumation process in a one-dimensional model can be addressed as follows:

(i) the high-pressure metamorphic units (MEU and GEU) being displaced are chosen as a reference coordinate system for the one-dimensional crustal section;

(ii) the vertical conductive heat transfer within the units is assumed to dominate the horizontal one (e.g. Fig. 10);
(iii) several discrete time segments are used to account for changes in the internal geometry of the migrating one-dimensional section during exhumation.

With this approach, a dynamic, one-dimensional model of the exhumation of metamorphic rocks in the Erzgebirge can be designed. In contrast to the simple "Jaeger-type" model (Jaeger, 1968) used by Werner and Lippolt (2000), this approach allows consideration of the influence of the individual P–T-time paths of each unit in the stack on the over all heat flow.

5.2. Specific model design and constraints

Model design and constraints (Fig. 17, Table 3) are based on the following key data for the Erzgebirge Dome (Willner et al., 2000; cf. Fig. 3):

- A thickened crustal bulge presumably existed for 60 Ma after the start of continent-continent collision at 400 Ma and before the onset of exhumation.
- The high-pressure rocks reached the surface about 15 Ma after the beginning of the exhumation process at ~340 Ma. Initial exhumation rates were high (~10 mm/a), decelerating with time during exhumation.
- Extensional deformation is preserved as penetrative fabrics imposed in the middle and upper crust and occurred concomitantly with stacking at depth.
- The amount of crust tectonically excised from the initial thickened crustal bulge exceeds 90%.

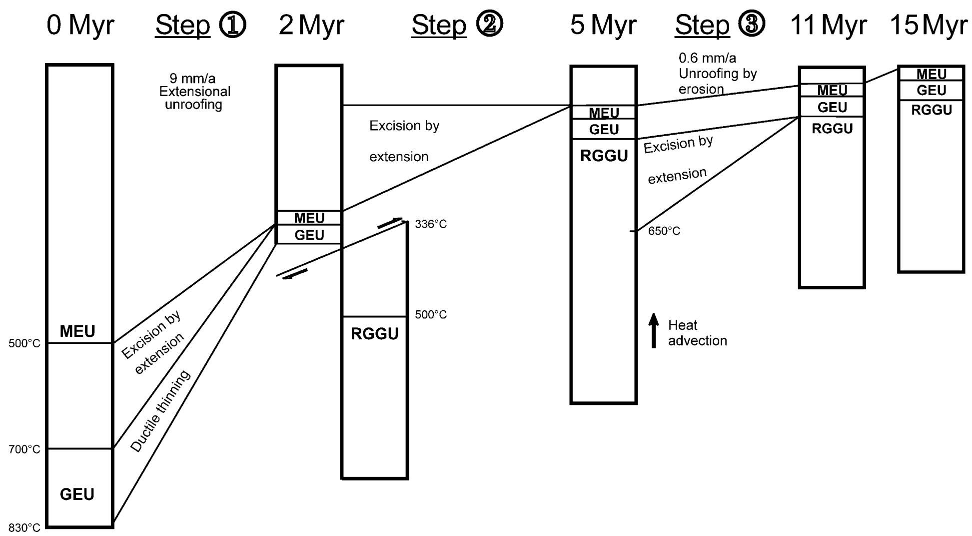

Fig. 17. Scheme of inferred stepwise juxtaposition of tectono-metamorphic units for the 1D-modelling of P–T-time paths of the Erzgebirge (cf. Table 3).

Table 3
Parameters of 1D numerical model

Boundary conditions	
Top	$T = 273$ K
Bottom	$q = 33.5 \cdot 10^{-3}$ W m^{-3}
Initial geotherm	$\partial T/\partial z = 0.012$ K m^{-1}
Average density of the crust, kg m^{-3}	2800
Heat conductivity, W m^{-1}K^{-1}	
Upper crust	1.75
Lower crust	1.50
Average heat production in the crust, W m^{-3}	$2 \cdot 10^{-6}$
Isobaric heat capacity, J kg^{-1}K^{-1}	
Upper crust	1100
Lower crust	1180

- Exhumation of high-pressure rocks occurred adjacent to an existing marine basin with thin crust. Turbiditic sedimentation was concomitant with deformation leading to the exhumation of the high-pressure rocks, i.e. considerable submarine relief was created at that time. However, considering the relatively small volume of detritus deposited in a short time, the role of erosion in exhumation (unroofing) was rather minor.
- During the late stages of exhumation, geothermal gradients increased considerably.
- Pb–Pb metamorphic zircon ages of 341 Ma (Kröner and Willner, 1998) and Ar–Ar-cooling ages of white mica around 340 Ma (Werner and Lippolt, 2000) point to initial exhumation rates in excess of 10 mm/a and cooling rates in excess of 50 °C/km.
- Resetting of Ar–Ar-ages around 330 Ma is observed in the GEU and possibly the MEU by Werner and Lippolt (2000) during a later stage of exhumation. An earlier 1D modelling by us (Willner et al., 1997a) could not take this constraint into account.

On the basis of these data, a general scheme for the exhumation history of the rocks of the Erzgebirge dome can be constrained (Fig. 17). The modelled P–T paths are assumed to be representative of the entire respective units. The best consistency between modelled and observed P–T paths (Fig. 18) was reached by considering a ~15 Ma duration of the following exhumation history.

5.2.1. Initial stage

Based on the preserved pressure maxima in all units (Fig. 5), a uniform initial geotherm of 12 °C/km was constructed, approximating the geothermal gradient existing after crustal stacking and at the beginning of exhumation around 341 Ma. A 75 km thick crust was chosen for a starting scenario. To simulate the curvature in the P–T paths (Fig. 5), three time segments with different exhumation rates (e.g. Figs. 13b and 14b) were modelled.

5.2.2. Time segment 1

A first 2 Ma was assumed for the interval of near-isothermal decompression between the pressure maximum and convergence of the MEU and the GEU in a mid-crustal level. During this

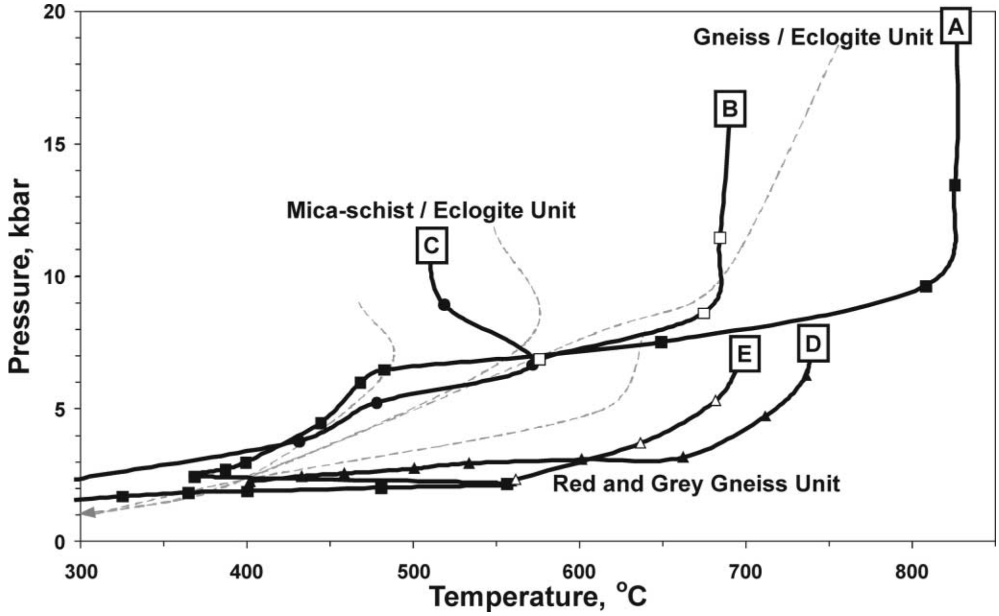

Fig. 18. Results of 1D modelling of P–T paths (solid lines) for the different metamorphic units of Erzgebirge: A—base of GEU; B—top of GEU; C—base of MEU; D—3 km below top of RGGU, E—top of RGGU. Observed P–T trajectories of metamorphic rocks of the Erzgebirge (Fig. 5) are shown by dashed gray lines.

interval the GEU is continuously stretched from an original 12 km to its present average thickness of around 3 km. The original thickness and a temperature difference of 700–830 °C between the top and bottom of the GEU was estimated from the initial transient geotherm of 12 °C/km. The crust between the present top of the GEU and the present base of the MEU is also continuously removed. For the upper crust an overall exhumation rate of 9 mm/a is proposed. The depth of convergence for both units in a mid-crustal level was deduced from Fig. 5.

5.2.3. Time segment 2

During a second time span of 3 Ma duration, both the MEU and the GEU cool below the 400 °C isotherm (to approximate the mineral cooling ages). A crust with a 12 °C/km transient geothermal gradient is thrust directly beneath the GEU at mid-crustal levels (336 °C at a depth of 28 km) causing rapid cooling from below and representing proposed underthrusting of the RGGU during exhumation of the high pressure units (see also the stacking of lower and upper crustal rocks in Fig. 10, 5.308 Myr). About 16 km of crust is continuously removed from the upper part of the MEU to reach the present 2 km thickness of this unit. This process is accompanied by cooling from an upper plate represented by the PU.

5.2.4. Time segment 3

To simulate partial resetting of cooling ages in the GEU and joint cooling with the RGGU, 14 km of crust are removed in 3 Ma between the present base of the GEU and a 25 km level (present top of the RGGU). The top of the RGGU is set at the beginning of this step to its maximum temperature of 650 °C, as derived from geothermobarometry. Emplacement of the RGGU at its thermal peak against the base of the GEU simulates penetrative extensional low-pressure deformation in the RGGU and cooling below 400 °C. A uniform exhumation rate of 0.6 mm/a is attained for all units, simulating erosion and exhumation of the top of the entire pile from a mid-crustal level to the surface within the last 10 Ma. Exhumation is accompanied by the cooling of the combined RGGU and GEU below 400 °C.

A summary of the physical parameters for the model is given in Table 3. Slight variations of these parameters were found to have no major effect on the results.

It should be emphasized that the above scenario, which is based on the actual P–T-time paths constructed for the various units (see summary in Willner et al., 2000), precludes a model such as that of Werner and Lippolt (2000), in which a relatively cool GEU is intercalated between mica schists of the MEU and the RGGU in physical contact at temperatures of 600 ± 50 °C.

5.3. Results

Our one-dimensional model was designed to be consistent with available knowledge on the sequence of tectonic events (Willner et al., 2000), geochronological data (Kröner and Willner, 1998; Werner and Lippolt, 2000) and P–T evolution (Willner et al., 1997b, 2000) of the metamorphic rocks of the Erzgebirge. Therefore, this model cannot be a priori considered to be an independent test of the validity of the delamination and detachment regime in the studied area. It does show, however, that geothermobarometry as well as 1D and 2D modelling converge into a consistent picture at all scales for the Bohemian Massif within the context of a delamination and detachment regime. The excellent consistency of the patterns of observed and numerically simulated P–T paths (Fig. 18) are evidence (Gerya et al., 2000) for the general validity of the absolute length of the assumed three rapid time segments of the exhumation process.

The following important relationships should also be mentioned.

1. Convergence of the reduced volumes of the MEU and the GEU during exhumation caused the decompression/heating leg of the P–T path of the MEU and the decompression cooling leg of the P–T paths of the GEU. The ~150 °C cooling of the GEU and the ~50 °C heating of MEU within the middle crustal level required less than 1 Ma, because of the significant reduction of the volumes of these units during the early near-isothermal decompression stage of the exhumation.
2. To yield the characteristic curvature of the P–T paths of the GEU and the MEU, the exhumation velocity of these units must be considerably lowered during the second stage of exhumation, i.e. from the mid-crustal level to the surface (see also Figs. 13 b, 14 b).
3. Resetting of Ar–Ar-ages as observed in the GEU and the MEU (Werner and Lippolt, 2000) can be considered to be the result of heating related to the underthrusting of the relatively hot RGGU (see the isobaric heating segment of the P–T path of the GEU at ~2 kbar in Fig. 18).

The one-dimensional model implies, in complete analogy to the two-dimensional models, that significant diversity of P–T paths for different metamorphic units is to be expected during the same relatively rapid tectonic process. Therefore, the different P–T-time paths should be treated as a genetic assemblage typical of a given geodynamic regime, and representing the tectono-metamorphic history of different rock units interrelated in space and time (Willner et al., 2000).

6. Summary and conclusion

According to the present study, the evolution of the continental crust during a continent-continent collision, delamination and full detachment process can be separated into three major stages.

6.1. Thickening of the crust

Thickening proceeds during a relatively long period (tens of Myr), including formation, delamination and detachment of the lithospheric bulge. This process may include rapid (within a few Myr) overthickening of the crust accompanying the last stage of the detachment process and the formation of a crustal wedge penetrating to a depth exceeding 160 km. After detachment, the crustal rocks forming the wedge are partially subducted together with the mantle lithosphere. However, a significant amount of wedge-forming material is returned to the base of the crust by buoyancy. This process of rapid overthickening of the crust may explain the occurrence of ultra-high-pressure rocks (garnet peridotites, eclogites, diamond-bearing gneisses) of uniform $\sim$340 Ma metamorphic age in the Bohemian Massif.

6.2. Extensional thinning of the crust

The thinning of the crust is caused by asthenosphere upwelling under the crustal bulge after detachment of the lithospheric mantle. This thinning is mainly related to the escape of the lower crustal rocks from the base of the crustal bulge towards the margins, characterized by the presence of weak tectonic zones. Most of the decompression of the lower crustal rocks occurs during this process. Horizontal displacement of lower crustal rocks may be of the order of 150–200 km and clearly exceeds the vertical displacement by a factor of $\sim$3. The lateral displacement is a maximum for the most deep-seated rocks and the exhumation velocity strongly decelerates with decreasing depth. This lateral displacement may explain the strong shearing and stacking of high-pressure metamorphic units during exhumation and extensional deformation. As follows from both geochronological data and the numerical modelling of P–T paths, the exhumation of high-pressure rocks to the middle crustal level proceeds relatively rapidly, i.e. within a few Myr.

6.3. Forced circulation within the crust

This process proceeds within weak tectonic zones (“exhumation channels”) at the margins of the crustal bulge and starts during the extensional stage. Weak zones represent former subduction zones or megascale intracrustal shear zones that originated during the collision process. Upward flow of lower crustal rocks occurs mainly in the hanging wall part of these zones and subduction of upper crustal rocks dominates in the foot wall. In both cases rocks from different depths amalgamate. The latter process may explain late stacking of lower and upper crustal units (GEU and RGGU) in a mid-crustal level. This circulation is associated with heating of the crust by underplating hot asthenosphere. This explains the late increase of the geotherm followed by the wide occurrence of late-orogenic S-type granites between about 330 and 320 Ma within the Erzgebirge dome and many other parts of the Bohemian massif. The highest increase of the geotherm is observed in these weak zones. The formation of the granites 10–20 Ma after exhumation is consistent with the characteristic time-scale (15–30 Ma) of appearance of crustal melts in cases of asthenospheric ascent up to a level immediately beneath the crust (Arnold et al., 2001).

Although the tectonic scheme outlined here is highly simplified, it appears to be in good agreement with the results of numerical experiments and the data on petrology and structural geology. This consistency in turn supports lithospheric delamination and full detachment (Schott and Schmeling, 1998) as the geodynamic regime causing the major features of Variscan ~340 Ma orogeny in the Bohemian Massif and particularly in the Erzgebirge dome, such as extremely rapid ascent of small amounts of UHP- and HP-rocks from the root of an ultra-thick crust.

Another important conclusion follows from the diversity of both the natural and modeled P–T-t-d-trajectories of different metamorphic units. P–T paths do not follow one single uniform exhumation trajectory and both decompression/cooling and decompression/heating P–T paths are characteristic. The diversity of P–T paths can be related to the diversity of the physical trajectories of the rocks in a non-homogeneous (both in time and space) thermal field, disturbed by rapid (5–30 mm/a) movement of mantle and crustal material. Therefore the diversity of P–T paths can be interpreted as a direct consequence of the relatively short (a few Myr) time-scale of geodynamic processes affecting the Bohemian Massif around ~340 Ma. For this type of process, assemblages of interrelated P–T-t-d paths (Willner et al., 2000) rather than a single-domain exhumation trajectory should be considered as representative for a specific geodynamic regime.

Acknowledgements

This research project was supported by grants from the Deutsche Forschungsgemeinschaft (Ma 689/11, SFB 526) and an Alexander von Humboldt Fellowship to TVG, which are gratefully acknowledged. The paper is also a contribution to the DFG priority programme "Modelling of orogenic processes with particular reference to the Variscides". We thank B. Schott, J. Arnold and W. Jacoby for long discussions and continuous support with 2D modelling as well as K. Klepeis, M. Kohn, K. Stüwe, H.-J. Massonne and two anonymous reviewers for detailed reviews and comments on various versions of the manuscript, stimulating its substantial revision.

References

Arnold, J., Jacoby, W.R., Schmeling, H., Schott, B., 2001. Continental collision and the dynamic and thermal evolution of the Variscan orogenic crustal root—numerical models. J. Geodynamics 31, 273–291.

Bird, P., 1978. Continental delamination and the Colorado Plateau. J. Geophys. Res. 84, 7561–7571.

Batt, G.E., Brown, J., 1997. On the thermomechanical evolution of compressional orogens. Geophys. J. Int. 128, 364–382.

Beaumont, C., Ellis, S., Hamilton, J., Fullsack, P., 1996. Mechanical model for subduction collision tectonic of Alpine-type compressional orogens. Geology 24, 675–678.

Blanckenbach, B., Busse, F., Christensen, U., Cserepes, L., Gunkel, D., Hansen, U., Harder, H., Jarvis, G., Koch, M., Marquart, G., Moore, D., Olson, P., Schmeling, H., Schnaubelt, T., 1989. A benchmark comparison for mantle convection codes. J. Geophys. Int. 98, 23–38.

Bousquet, R., Goffe, B., Henry, P., Le Pichon, X., Chopin, C., 1997. Kinematic, thermal and petrological model of the Central Alps: Lepotine metamorphism in the upper crust and eclogitisation of the lower crust. Tectonophys. 273, 105–127.

Carswell, D.A., 1991. Variscan high P–T metamorphism and uplift history in the Moldanubian zone of the Bohemian Massif, Lower Austria. Eur. J. Mineral. 3, 323–342.

Carswell, D.A., O'Brien, P.J., 1993. Thermobarometry and geotectonic significance of high-pressure granulites: examples from the Moldanubian zone of the Bohemian Massif in Lower Austria. J. Petrol. 34, 427–459.

Chemenda, A.I., Matte, P., Sokolov, V., 1997. A model of Paleozoic obduction and exhumation of high-pressure/low-temperature rocks in the southern Urals. Tectonophysics. 276, 217–227.

England, P.C., Thompson, A.B., 1984. Pressure-temperature-time paths of regional metamorphism; I, Heat transfer during the evolution of regions of thickened continental crust. J. Petrol 25, 894–928.

Ernst, W.G., Peacock, S.M., 1996. A thermotectonic model for preservation of ultrahigh-pressure phases in metamorphosed continental crust. In Behout, G.E., Scholl, D.W., Kirby, S.H and Platt, J. (Eds.), Subduction—Top to Bottom. AGU Geophysical Monograph 96, 171-178.

Franke, W., Stein, E., 2000. Exhumation of high-grade rocks in the Saxo-Thuringian Belt: geological constraints and geodynamic concepts. In: Franke, W., Haak, V., Oncken, O., Tanner, D. (Eds.), Orogenic Processes: Quantification and Modelling in the Variscan Belt, Vol. 197. Spec. Pub. Geol. Soc. London, pp. 179, 337–354.

Gerya, T.V., Perchuk, L.L., van Reenen, D.D., Smit, C.A., 2000. Two-dimensional numerical modelling of pressure-temperature-time paths for the exhumation of some granulite facies terrains in the Precambrian. J. Geodynamics 30, 17–35.

Houseman, G.A., England, P.C., 1986. Finite strain calculations of continental deformation 1. Method and general results for convergent zones. J. Geophys. Res. 91, 3651–3663.

Houseman, G.A., McKenzie, D.P., Molnar, P., 1981. Convective instability of a thickened boundary layer and its relevance for the thermal evolution of continental convergent belts. J. Geophys. Res. 86, 6115–6132.

Jaeger, J.C., 1968. Cooling and solidification of igneous rocks. In: Hess, H.H., Poldervaart, A. (Eds.), Basalts. The Poldervaart treatise on rocks of basaltic composition. Vol. 2. John Wiley & Sons, New York, pp. 503–536.

Klemm, I., 1995. Druck-Temperaturentwicklung von Metamorphiten im östlichen Erzgebirge (Sachsen). Unpubl. diploma thesis Univ. Bochum (Germany), 121 pp.

Kotkovà, J., Harley, S.L., Fisera, M., 1997. A vestige of very high-pressure (ca. 28 kbar) metamorphism in the Variscan Bohemian Massif, Czech Republic. Eur. J. Mineral. 9, 1017–1033.

Koyi, H.A., Milnes, A.G., Schmeling, H., Talbot, C.J., Zeyen, H., 1999. Numerical models of ductile rebound of crustal roots beneath mountain belts. Geophys. J. Int. 139, 556–562.

Krohe, A., 1998. Extending a thickened crustal bulge: toward a new geodynamic evolution model of the paleozoic NW Bohemian Massif, German Continental Deep Drilling site (SE Germany). Earth-Sci. Review 44, 95–145.

Kröner, A., Willner, A.P., 1998. Time of formation and peak of Variscan HP-HT metamorphism of quartz-feldspar rocks in the central Erzgebirge, Saxony, Germany. Contrib. Mineral. Petrol 132, 1–20.

Kröner, A., O'Brien, P.J., Nemchin, A.A., Pidgeon, R.T., 2000a. Zircon ages for high pressure granulites from South Bohemia, Czech Republic, and their connection to Carboniferous high temperature processes. Contrib. Mineral. Petrol. 138, 127–142.

Kröner, A., O'Brien, P.J., Nemchin, A.A., Pidgeon, R.T., 2000b. Zircon ages for high pressure granulites from South Bohemia, Czech Republic, and their connection to Carboniferous high temperature processes. Contrib. Mineral. Petrol. 138, 127–142.

Kryza, R., Pin, C., Vielzeuf, D., 1996. High-pressure granulites from the Sudetes (south-west Poland): evidence of crustal subduction and collisional thickening in the Variscan belt. J. Metam. Geol. 14, 531–546.

Massonne, H.-J., 1992. Thermochemical determination of water activities relevant to eclogitic rocks. In: Kharaka, Y.K., Maest, A.S. (Eds.), Water–rock Interaction. Proceedings of the 7th Intern. Symp. on Water-Rock Interaction, Park City, Utah. Rotterdam, Balkema, pp. 1523–1526.

Massonne, H.-J., 1999. A new occurrence of microdiamonds in quartzofeldspathic rocks of the Saxonian Erzgebirge, Germany, and their metamorphic evolution. In: Gurney, J.J., Gurney, J.L., Pascoe, M.D., Richardson, S.H. (Eds), The P.H. Nixon Volume Proceedings 7th International Kimberlite Conference, Cape Town, Vol. 2, pp. 533–539.

Massonne, H.-J., 2001. First find of coesite in the ultrahigh-pressure metamorphic area of the central Erzgebirge, Germany. Eur. J. Mineral. 13, 565–570.

Mengel, K., 1992. Integrated lithospheric cross section. In: Blundell, D. (Ed.), A Continent Revealed: The European Geotraverse 1. Cambridge University Press, Reading, pp. 102–110.
O'Brien, P., Carswell, D.A., 1993. Tectonometamorphic evolution of the Bohemian Massif: evidence from high pressure metamorphic rocks. Geol.Rundsch. 82, 531–555.
Peacock, S.M., 1989. Thermal modelling of metamorphic pressure-temperature-time paths: a forward approach. In: Spear, F.S., Peacock, S.M. (Eds.), Metamorphic Pressure-Temperature-Time Paths, Vol. 7. AGU Short Course in Geology, pp. 58–102.
Perchuk, A.L., Philippot, P., Erdmer, P., Fialin, M., 1999. Rates of thermal equilibration at the onset of subduction deduced from diffusion modelling of eclogitic garnets, Yukon-Tanana terrain. Geology 27, 531–534.
Perchuk, L.L., 1989. P–T-fluid regimes of metamorphism and related magmatism with specific reference to the Baikal Lake granulites, in: Daly, S., Yardley, D.W.D., Cliff, B. (Eds.), Evolution of Metamorphic Belts. Geol. Soc. London, Spec. Publ., pp. 275–291.
Platt, J.P., England, P.C., 1993. Convective removal of lithosphere beneath mountain belts: thermal and mechanical consequences. Am. J. Sci. 293, 307–336.
Pysklywec, R.N., Beaumont, C., Fullsak, P., 2000. Modeling the behavior of the continental mantle lithosphere during plate convergence. Geology 38, 655–658.
Ranalli, G., 1995. Rheology of the Earth, 2nd ed. Chapman and Hall, London.
Reinhardt, J., Kleemann, U., 1994. Extensional unroofing of granulitic lower crust and related low pressure/high temperature metamorphism in the Saxonian Granulite Massif, Germany. Tectonophys. 238, 71–94.
Rötzler, K., Schumacher, R., Maresch, W.V., Willner, A.P., 1998. Characterization and geodynamic implications of contrasting metamorphic evolution in juxtaposed high-pressure units of the Western Erzgebirge (Saxony, Germany). Eur. J. Min 10, 261–280.
Sandiford, M., Powell, R., 1990. Some isostatic and thermal consequences of the vertical strain geometry in convergent orogens. Earth Planet. Sci. Lett. 98, 154–165.
Schmädicke, E., Okrusch, M., Schmidt, W., 1992. Eclogite-facies rocks in the Saxonian Erzgebirge, Germany: High pressure metamorphism under contrasting P–T conditions. Contrib. Mineral Petrol. 110, 226–241.
Schmeling, H., 1989. Compressible convection with constant and variable viscosity: the effect on geoid, topography and slab deformation. J. Geophys. Res. 94, 12463–12481.
Schmeling, H., Bussod, G.Y., 1996. Variable viscosity convection and partial melting in the continental asthenosphere. J. Geophys. Res. 101, 5411–5423.
Schmeling, H., Marquart, G., 1991. The influence of second-scale convection on the thickness on continental lithosphere and crust. Tectonophys 189, 281–306.
Schott, B., Schmeling, H., 1998. Delamination and detachment of a lithospheric root. Tectonophys. 296, 225–247.
Schott, B.D., Yuen, A., Schmeling, H., 2000. The significance of shear heating in continental delamination. Phys. Earth Planet. Interior 118, 273–290.
Spear, F.S., 1993. Metamorphic phase equilibria and pressure-temperature-time paths. Min. Soc. Am. Publication, Washington, DC.
Stöckhert, B., Duyster, J., Trepmann, C., Massonne, H.-J., 2001. Microdiamond daughter crystals precipitated from supercritical COH silicate fluids included in garnet, Erzgebirge, Germany. Geology 29, 391–394.
Stüwe, K., Barr, T.D., 1998. On uplift and exhumation during convergence. Tectonics 17, 80–88.
Stüwe, K., Sandiford, M., 1995. Mantle-lithospheric deformation and crustal metamorphism with some speculations on the thermal and mechanical significance of the Tauern Event, Eastern Alps. Tectonophys. 242, 115–132.
Tichomirova, H., Belyatski, B.V., Berger, H.J., Koch, E.A, 1996. Geochronological investigations on grey gneisses from the Freiberg Region (Eastern Erzgebirge). J. Conf. Abstracts 1 (1), 620.
van Keken, P.E., King, S.D., Schmeling, H., Christensen, U.R., Neumeister, D., Doin, M.P., 1997. A comparison of methods for the modelling of thermomechanical convection. J. Geophys. Res. 102, 22477–22495.
Werner, O., Lippolt, H.J., Hess, J.C., 1997. Isotopische Randbedingungen zur Bestimmung der Alter tektonischer Prozesse im variszischen Erzgebirge. Terra Nostra 97/ 5, 199–203.
Werner, O., Lippolt, H.J., 2000. White mica $^{40}Ar/^{39}Ar$ ages of Erzgebirge metamorphic rocks: simulating the chronological results by a model of Variscan crustal imbrication. In: Franke, W., Haak, V., Oncken, O., Tanner, D. (Eds.). Orogenic Processes: Quantification and Modelling in the Variscan Belt, Vol. 179. Spec. Pub. Geol. Soc. London, pp. 323–336.

Willner, A.P., Klemm, I., Rötzler, K., Maresch, W.V., 1995. Petrologische Belege aus dem mittelkrustalen Niveau für eine variskische Krustenstapelung im Erzgebirge. Terra Nostra. 95 (8), 138.

Willner, A.P., Jacoby, W., Klemm, I., Krohe, A., Kröner, A., Kopp, J., Maresch, W.V., Rötzler, K., Schumacher, R., Sebazungu, E., 1997a. Krustendynamik im variszischen Erzgebirge (Sachsen): Ein Modell für die Exhumierung von ultratiefer Kruste in Kollisionsorogenen. Terra Nostra 97 (5), 208–211.

Willner, A.P., Rötzler, K., Maresch, W.V., 1997b. Pressure-temperature and fluid evolution of quartzo-feldspathic metamorphic rocks with a relic high-pressure, granulite-facies history from the Central Erzgebirge (Saxony, Germany). J. Petrol. 38, 307–336.

Willner, A.P., Krohe, A., Maresch, W.V., 2000. Interrelated P–T-t-d- paths in the Variscan Erzgebirge Dome (Saxony/Germany): constraints on the rapid exhumation of high pressure rocks from the root zone of a collisional orogen. Intern. Geol. Reviews 42, 64–85.

Zhou, S., Sandiford, M., 1992. On the stability of isostatically compensated mountain belts. J. Geophys. Res. 97, 14207–14221.

Zulauf, G., 1997. Von der Anchizone bis zur Eklogitfazies: Angekippte Krustenprofile als Folge der cadomischen und variszischen Orogenese im Tepla-Barrandium (Böhmische Masse). Geotektonische Forschungen 89, 1–302.